



Journal homepage: <http://civiljournal.semnan.ac.ir/>

Liquefaction Susceptibility Mapping in West Bengal with Emphasis on its Capital City Kolkata under the Impact of a Few Great Earthquakes Triggered from the Himalaya and Northeast India

S. K. Nath^{1*}, C. Ghatak¹, A. Biswas¹, A. Srivastava¹

1. Department of Geology and Geophysics, Indian Institute of Technology Kharagpur, India

Corresponding author: nath@gg.iitkgp.ac.in

ARTICLE INFO

Article history:

Received: 30 July 2021

Revised: 09 December 2021

Accepted: 17 December 2021

Keywords:

Liquefaction;

Factor of Safety;

Probability of liquefaction;

Liquefaction Risk.

ABSTRACT

A host of great historical earthquakes from the Himalayas and Northeast India reportedly triggered liquefaction with the surface manifestation of sand boil, ground subsidence and lateral spreading in West Bengal and its capital city Kolkata located in the alluvium-rich Ganga-Brahmaputra river system, thus presenting a strong case towards systematic liquefaction potential analysis for this terrain using multivariate techniques based on a large Geophysical and Geotechnical data base. An integrated computational protocol has provided site classification of the terrain following standard nomenclature and its characterization in terms of absolute and generic spectral site amplification through equivalent linear/ non-linear geotechnical response spectral modelling as an intermediate step towards Liquefaction Potential and Risk assessment of the region. The large Geotechnical database is used for estimating Cyclic Stress Ratio (CSR) and Cyclic Resistance Ratio (CRR), which further delivered Factor of Safety (FOS), Liquefaction Potential Index (LPI), Probability of Liquefaction (PL), and Liquefaction Risk Index (IR) in the State and its capital Kolkata. The State including Kolkata have been classified into 'Severe', 'High', 'Moderate' and 'Non-liquefiable' zones based on LPI distribution while the liquefaction risk map classified the terrain into 'Low ($IR \leq 20$)', 'High ($20 < IR \leq 30$)' and 'Extreme ($IR > 30$)' Risk Zones. An intensely liquefiable stratum with $FOS < 1$ is identified in the 5-15m depth region consisting of coarse-grained variants of sand, silty-sand and clayey-silty sand with an approximately 0.5-12.7m deep groundwater condition. An understanding of the liquefaction potential and its associated risk will act as catalyst in reducing structural vulnerability of the terrain by improving sediment strength.

How to cite this article:

Nath, S., Ghatak, C., Biswas, A., Srivastava, A. (2022). Liquefaction Susceptibility Mapping in West Bengal with emphasis on its Capital City Kolkata under the Impact of a few Great Earthquakes triggered from the Himalaya and Northeast India. *Journal of Rehabilitation in Civil Engineering*, 10(4), 56-96.

<https://doi.org/10.22075/JRCE.2021.24034.1533>

1. Introduction

The impact of large earthquakes on an alluvium-rich terrain causes soil/sediment to act like a viscous fluid due to increased pore water pressure caused by the compaction of granular deposits, wherein soil/sediment loses its bearing capacity under the impact of these large earthquakes as evidenced by several historical earthquakes around the globe viz. the 18 April 1906 San Francisco earthquake, 01 September 1923 Kwanto earthquake, 18 April 1928 Bulgarian earthquake, 18 May 1940 Imperial Valley earthquake, 17 October 1989 Loma Prieta earthquake, 17 January 1995 Kobe earthquake [1] and many such large earthquakes that exhibited ejection of sand and water, ground subsidence and lateral spreading resulting from liquefaction phenomenon due to reduction in shear resistance caused by monotonic, cyclic or shock loading [2, 3]. In San Francisco, lateral spreading during the 1906 earthquake and the 1989 earthquake caused severe damage in the region. The 1964 Great Alaskan earthquake of Mw 9.2 and Niigata earthquake of Mw 7.6 caused intensive liquefaction induced bridge and building foundation failure, slope failure, and floatation of buried structures [4, 5]. The 1994 Northridge California earthquake of Mw 6.7 also exhibited liquefaction-induced cracks and permanent ground deformation [6]. Ground fissures and sand boils have been observed during the 2003 Lefkada earthquake of Mw 6.2 [7]. Shahri et al [8] used C# GUI code “NLGSS_Shahri” to calculate soil liquefaction potential of Nemat Abad Dam of Iran considering the impact of 2002 Avaj-Chanugureh earthquake (m_b 6.5) based on geological and geotechnical database. In India, the states of Assam,

Meghalaya, West Bengal and the northern part of Bangladesh observed large-scale land deformation with outburst of sand and water, lateral spreading, and mud volcanic eruptions during the 1897 Shillong earthquake of Mw 8.1 having catastrophic effects on urban structures [1, 9]. Thus 1897 Shillong earthquake that nucleated in a steep south-southeast-sloping thrust fault under the northern boundary of central Shillong thus holding a significant place in the history of the greatest earthquakes of the Indian subcontinent [10]. The 1918 Srimangal earthquake of Mw 7.6 is counted as one among the largest earthquakes that has severely affected the Bengal Basin. The jolting due to this earthquake was felt in a large area of $\sim 74000\text{km}^2$ extending up to Kathmandu in the north, Rangoon in the south, Manipur in the east, and Kolkata in the west [11]. Huge cracks, fissures and landslides were observed near the epicenter [12]. The 10 January 1869 Cachar earthquake of Mw 7.4 and 10 August 1950 Assam earthquake of Mw 8.7 also exhibited heavy damages due to liquefaction near the epicentral region [10]. Building collapse, ground failure, fractures, tilting of structure and explosion of water, peat and sand in the north of the River Ganges were narrated during the 15 January 1934 Bihar-Nepal earthquake of Mw 8.1 [13]. The 2015 Gorkha Nepal earthquake of Mw 7.8 nucleated from the subduction zone between the Indian plate and the Eurasian plate along the Himalayan arc exhibited widespread liquefaction with surface manifestation of sand boils and fissures and destroyed 138,182 houses across Nepal and its adjoining region. A brief review of the devastations inflicted by these large to great earthquakes on West Bengal, as well as Kolkata, their liquefaction signatures

and the damage and destruction reported in various literatures is presented in Table 1[14-25].

The present investigation aims at performing systematic liquefaction susceptibility assessment in terms of Factor of Safety (FOS), Probability of Liquefaction (P_L), Liquefaction Potential Index (LPI) and Liquefaction Risk Index (I_R) in the state of West Bengal with special emphasis on its capital city Kolkata under the influence of a few of these great earthquakes in an attempt towards understanding nonlinear soil-structure interaction dynamics so as to put in place appropriate foundation measures.

2. Study region

The state of West Bengal is a shelter of 100 million people with the highest concentration in its capital city of Kolkata. The most significant tectonic feature in the State is the 25km wide, NE–SW trending Eocene Hinge Zone (EHZ) also called the Calcutta–Mymensingh Hinge Zone, extending to a depth of ~4.5km below Kolkata. An earthquake of Mw 6.2 in 1935 reportedly originated from EHZ and was felt in and around Kolkata. The 1964 Sagar Island earthquake of Mw 5.4 also felt in Kolkata on focal mechanism solution suggested thrust mechanism with minor strike slip component [21]. The other significant tectonic features of this terrain are the Jangipur–Gaibandha Fault, Garhmoyna–Khandaghosh Fault, Debagram–Bogra Fault, Pingla Fault, Malda–Kishanganj Fault, Rajmahal Fault, Purulia Shear Zone, Sainthia–Bahmani Fault, Main Central Thrust, Main

Boundary Thrust, Tista Lineament, and Purulia Lineament. The entire state of West

Bengal stretching over 88,752km² with a population density of 1028 per km² is exposed to probable seismic threat from the major Northeastern fault system comprising of Dauki, Oldham and Dhubri Faults and from the Himalayas to its north. The seismotectonic setting of West Bengal and its surrounding along with major earthquake epicenters depicted in Figure 1 suggests that the Shillong plateau and the subduction zone of the Himalaya are the major contributors to the seismicity of the region.

West Bengal is bestowed with wide expanses of alluvial plains extending from the Himalaya to the Bay of Bengal[27, 28]. Rugged hills and valleys dominate the Himalayan region in the northern district of Darjeeling consisting primarily of Archean Gneisses and Plio-Pleistocene sedimentary formation. The sub-Himalayan alluvial fans, majorly Tista megafan of the districts of Jalpaiguri, Alipurduar, Coochbehar and Uttar Dinajpur have Pleistocene to Holocene gravelly sand and silt. The Barind uplands of Malda and Dakshin Dinajpur are covered with oxidized clay and silt of Pleistocene age. The northern zone is filled with channels and small streams due to the tributaries of the Brahmaputra and Ganges Rivers. The western extremity of West Bengal originated as the coastal part of the Northeastern Indian craton that evolved from the Gondwanaland in Early Cretaceous and eventually drifted northwards. The degenerated eastern fringes of the Chhotanagpur plateau in the districts of Puruliya and the western part of the Bankura, Paschim Bardhaman, Birbhum and Jhargram consist of Proterozoic gneiss and other metamorphics. The plateau fringe palaeodeltas or the western fan system is known by the name of Rarh plains in the lateritic western districts of West Bengal.

Table 1. A few large earthquakes that have inflicted liquefaction phenomenon and severely affected the state of West Bengal have been listed together with their source attributes and the extent of damage inflicted by those on the state of West Bengal and its capital city Kolkata.

Sl No.	Year of nucleation of the Earthquake	Magnitude M_w	Latitude ($^{\circ}$ N)	Longitude ($^{\circ}$ E)	Focal Depth (km)	Epicentral Distance from the capital city of Kolkata (m)	Liquefaction Signature evidenced at and near the source region	MM Intensity felt in Kolkata	Impact of the earthquake in State of West Bengal	Reference
1	1897	8.1	26.0	91.1	35	460.28	Sand Boils, Mud Volcanoes, Fissures, Ground Subsidence	IV-V	Structural Damage at Harrington Street and Circular Road in Kolkata. A number of houses were damaged in Darjeeling Most brick houses were damaged beyond repair in Cooch Behar. Many other places across the Bengal also have been reported to have little damage.	[1, 9, 10, 14, 16]
2	1918	7.6	24.5 $^{\circ}$ N	91.0	14	350.07	Sand Spouting, Fissures	IV	Ominous cracks in buildings in Clive Street, College Street and Shyambazar of Kolkata.	[17]
3	1930	7.1	25.5	90.0	60	360.02	Fissure with sand and water spouting, Ground Subsidence	IV	Old brick buildings were badly shattered and in some cases partially collapsed in Cooch Behar. North abutment of Gitaldaha Junction was severely cracked. Masonry structures including the Court building and offices were reported to have been badly cracked in Alipurduar. Minor cracks in well-built structures were observed in other places.	[18, 19]
4	1934	8.1	25.5	90.0	20	420.17	Sand Boil, Fissures, slump zone, Ground subsidence	VI-VII	Structural damage and ominous cracks, Ground subsidence has been reported as prominent liquefaction signature at Park Street, Kolkata. Ichhapur of Howrah also has been reported to suffer from minor damage.	[13]
5	1950	8.7	24.25	89.5	50	1000	Sand Boils	III-IV	Shaking of buildings and other structure were reported.	[21, 22]
6	1988	6.8	26.72	86.62	64.6	400	Sand Vents, Fissures, Ground Subsidence	IV	Shaking of building and other structures.	[23]
7	2011	6.9	22.72	88.06	47	570	Fissures, Lateral Spreading, Ground Subsidence	III-IV	Cracks developed in the buildings and in the road.	[24]
8	2015	7.8	28.17	84.70	8.2	700	Sand Boils, Lateral Spreading, Fissures, Ground Subsidence	IV	Minor Cracks in the metal road observed.	[25]; News Reporting.

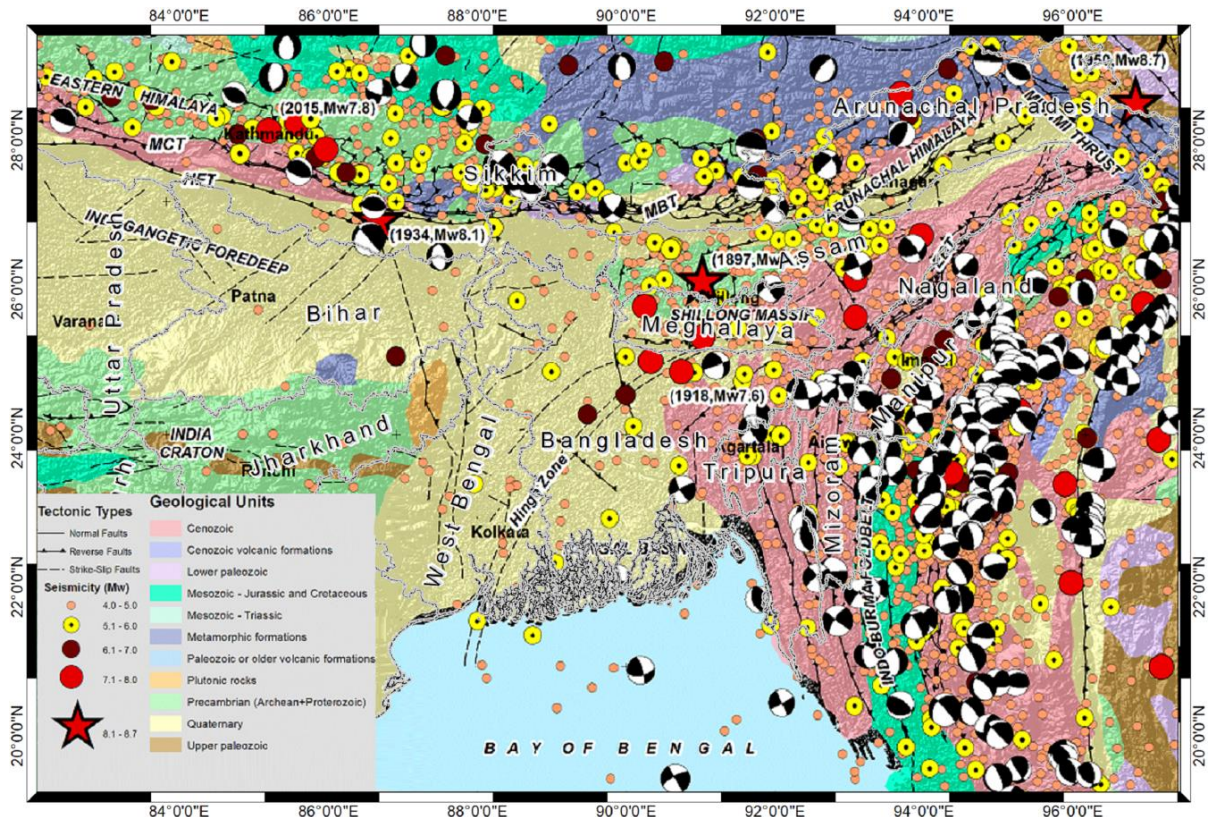


Fig. 1. Seismotectonic setting of Bengal Basin and its surrounding region [21] with the epicenters of significant earthquakes of $M_w \geq 4.0$ shown on the map [26].

The east-flowing rivers of the State *viz.* the Mayurakshi, the Ajay, the Damodar, the Rupnarayan and the Kangsabati-Haldi contributed to the collated deltas joining the Ganges-Brahmaputra delta. The primarily non-tidal upper Ganges delta with Holocene younger alluvium contains levees, floodplains, back swamps and paleochannels. The tidal lower Ganges delta occupied by the Sundarbans mangroves is majorly filled with Holocene deposits like tidal silt and clay, sand in channels or beaches of islands. The Medinipur coastal plains with Holocene coastal deposits have Chenier beach ridges in the west and small palaeo-channels with levees in the east. Distributaries of the Ganges and tributaries of Bhagirathi-Hugli

have drained the southern part of the State. Clearly, most of the areas reside over thick younger alluvium composed of shallow layers of silt, clay and sand, which can be disastrous in terms of site amplification and liquefaction if any strong ground shaking takes place.

Kolkata, the most important city in terms of population, administration, urban infrastructure and heritage and the capital of West Bengal, have emerged along the southern part of Hugli River, the westernmost distributary of the River Ganges and bounded by several canals like Bagjola Khal in the north and Beliaghat and Circular Khal in the middle and the palaeochannel Adi-Ganga, and Talli nala in the south.

Having the Bay of Bengal coastline only 100km and Sundarbans only 60km away, geomorphologically Kolkata is dominated by deltaic plain with elevation ranging from 3.5 to 6m above Mean Sea Level and a southward slope. In addition, there are several interdistributary marsh, paleochannels and younger levee adjacent to river Hugli and older levee on both sides of the old Adi Ganga present in the area. Two major geologic units are observed in the City namely middle to late Holocene Panskura

formation comprising of sands, silts, and meander scrolls along the banks of River Hugli, and late Holocene Hugli formation with loose unconsolidated grey fine to coarse sand and gravel in rest of the City. It has sequence of stratigraphy as Quaternary deposit, Tertiary sediments, Cretaceous trap and Permo-Carboniferous Gondwana rocks from top to bottom. The Geology-Geomorphology maps of West Bengal and the city of Kolkata are depicted in Figure 2.

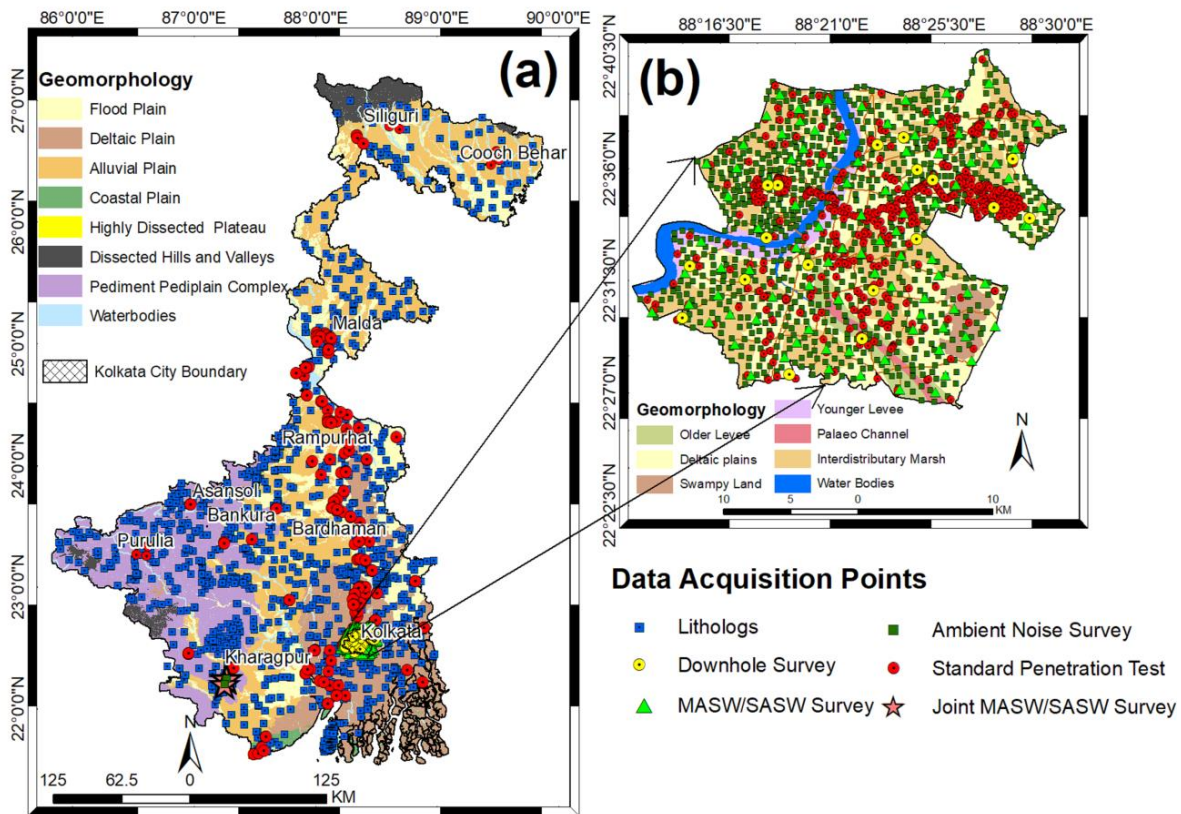


Fig. 2. Geology-Geomorphology map of West Bengal and Kolkata shown in (a) and (b) respectively (https://bhuvan.nrsc.gov.in/bhuvan_links.php). The Geophysical, Lithological and Geotechnical Data Acquisition sites are also marked on both the maps [29].

3. Data

In order to delineate the inherent characteristics, sequence and thickness of subsurface strata and to determine the corresponding engineering properties that

measure the soil strength, composition, density, water content and other physical and lithological properties intended for site classification and its characterization for the vast seismogenic tectonic study region, extensive surface measurements have been carried out in the form of Ambient Noise Survey, Spectral Analysis of Surface Waves (SASW), Multi-channel Analysis of Surface Waves (MASW), Joint Microtremor & MASW Data Acquisition & Processing and in-situ measurements through Downhole Seismic Survey, Standard Penetration Test and Geotechnical Investigations involving bulk density estimation, unit weight, moisture content, fine content, Atterberg limit tests (PL, LL), grain size analysis etc. In the present investigation at around 5000 locations both the surface and in-situ measurements have been conducted as shown in Figure 2 for the estimation stratum-wise effective shear wave velocity and establish its spatial distribution thus accomplishing site classification of the terrain considering the top 30m sediment cover.

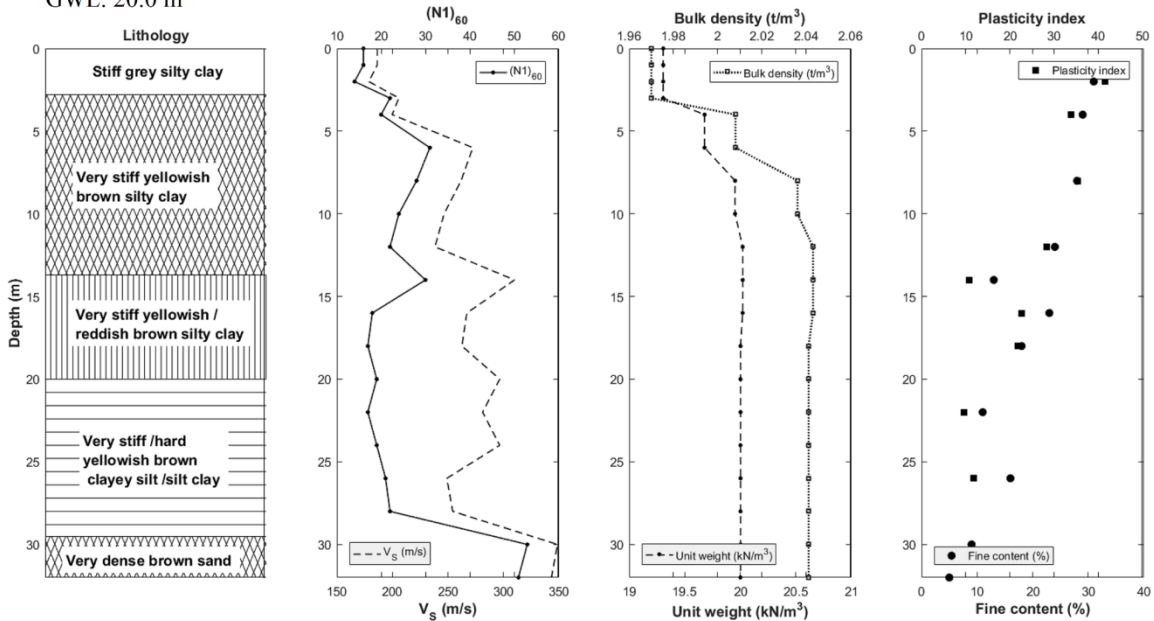
3.1. Invasive geotechnical investigation

Geotechnical investigations incorporate drilling, soil sampling, and

laboratory tests to conduct subsurface in-situ exploration at various sites. The aim of an in-situ site investigation is to determine reliable subsurface properties of soil/rock through drilling techniques, which play important role in seismic design of safe urban structures. The Static Cone Penetration Test (SCPT), Dynamic Cone Penetration Test (DCPT), and the Standard Penetration Test (SPT) are the most commonly used in-situ soil testing tools. SPT is a complex in-situ penetration test for

determining the geotechnical engineering properties of soil like compactness of cohesive and non-cohesive soil types etc. SPT has been conducted in the present study at 1.5m interval to estimate soil stiffness, physical and shear parameters and N values of all the lithological units encountered during the drilling. However, before further use field acquired SPT-N values are corrected [3]. Some representative corrected SPT-N $[(N_1)_{60}]$ borehole data for West Bengal are shown in Figure 3, while that for Kolkata are shown in Figure 4.

(a) Location: Sagardighi Thermal Power Station, Monigram, Murshidabad (24°20'15"N, 88°12'4.6"E)
 GWL: 20.0 m



(b) Location: Haldia Energy Power Station, Jhikurkhal, Haldia (22°6'12.8"N, 88°10'35.4"E)
 GWL: 0.80 m

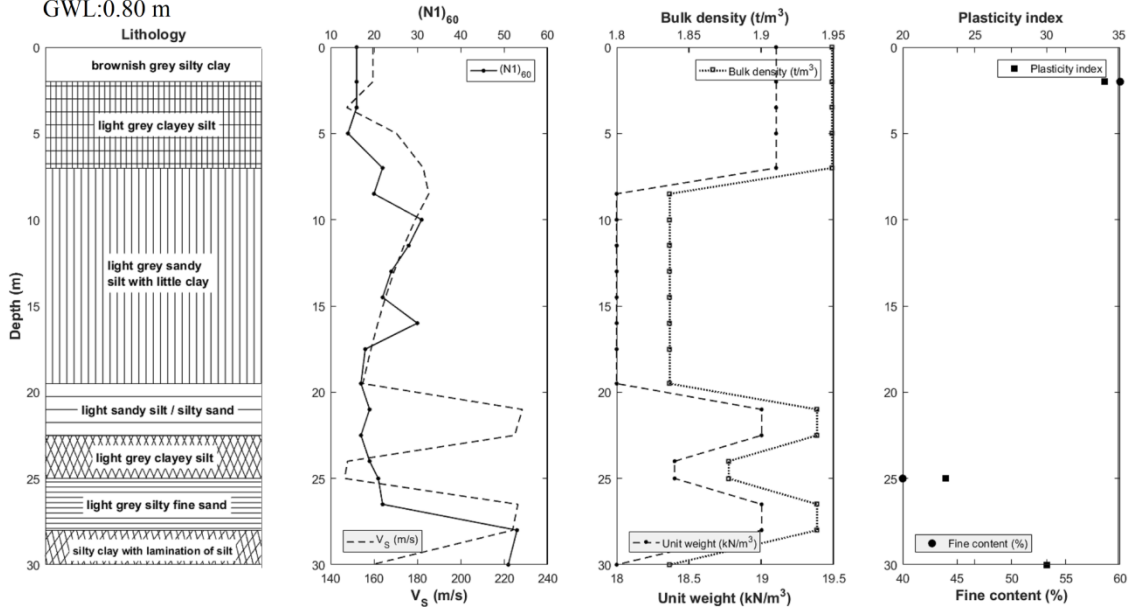


Fig. 3. Representative Geotechnical Borehole dataset with depth-wise lithology, (N1)60, SPT derived Shear wave Velocity, Unit Weight, Plasticity Index at Murshidabad and Haldia in West Bengal.

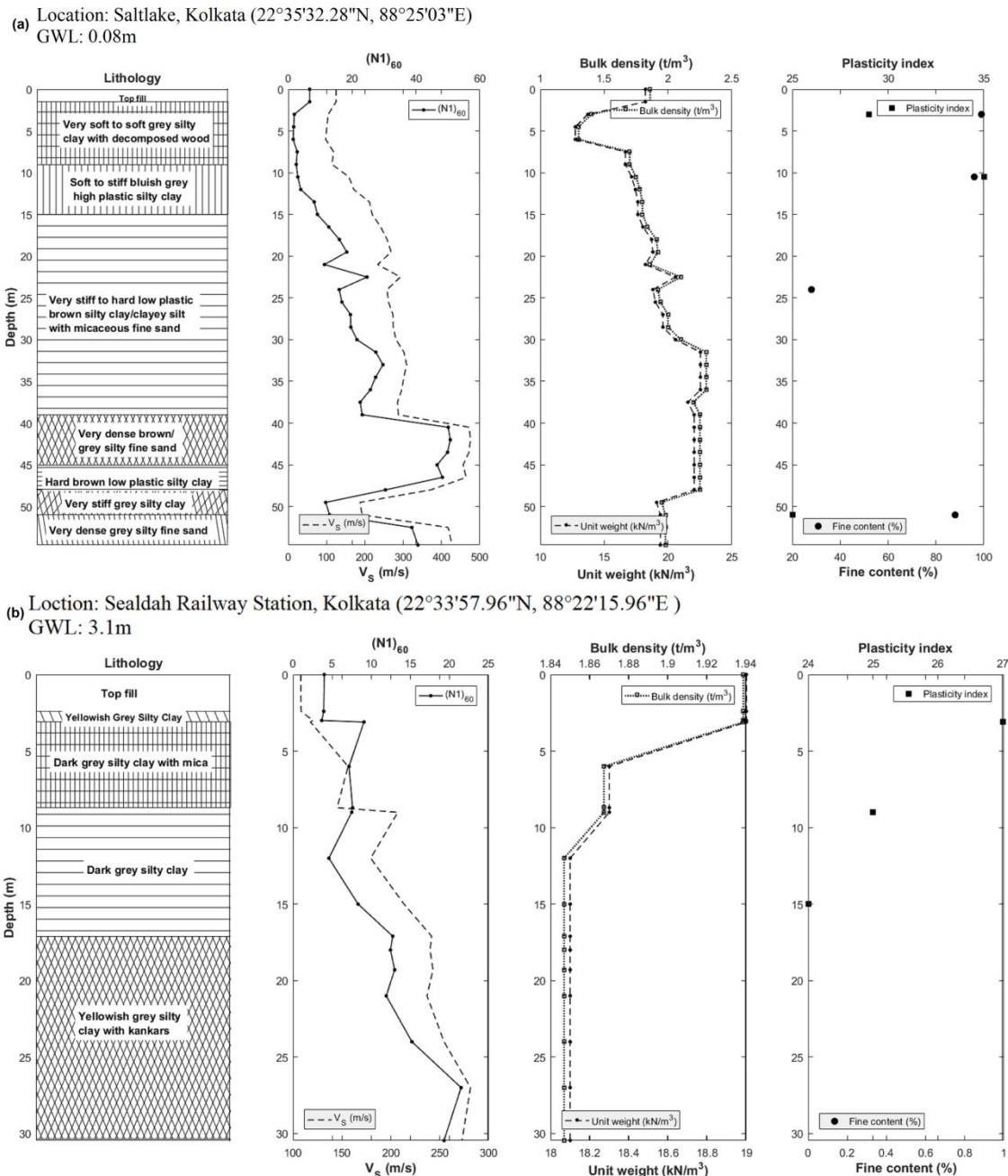


Fig. 4. Representative Geotechnical Borehole dataset with depth-wise lithology, $(N_1)_{60}$, SPT derived Shear wave velocity, Unit Weight, Plasticity Index at Saltlake City and Sealdah Railway Station in Kolkata.

3.2, Invasive downhole seismic survey

The primary goal of a downhole seismic test is to determine the shear wave velocity (V_s) as well as dynamic soil parameters such as the Poisson's ratio, bulk modulus, shear

modulus, and young modulus. This technique uses a 3-component geophone to calculate vertical changes in seismic velocity by positioning a source at the top of a borehole and calculating travel times of signals from an impulsive source of energy at the surface

to a series of measurement points in the borehole. The shear wave velocity (V_s) is calculated by dividing the difference between the distances covered by the S-waves, assuming a linear direction, by the time interval as given in Eq. 1

$$V_s = \frac{L_2 - L_1}{T_2 - T_1} \quad (1)$$

Where, $T_2 - T_1$ is the difference between the arrival times of seismic waves to the transducers at two distances (L_1 and L_2) of the seismic source and L_1 & L_2 are the first and second transducer distances from the source, respectively. Representative Downhole test dataset from West Bengal and Kolkata have been presented in Figures 5 and 6 respectively.

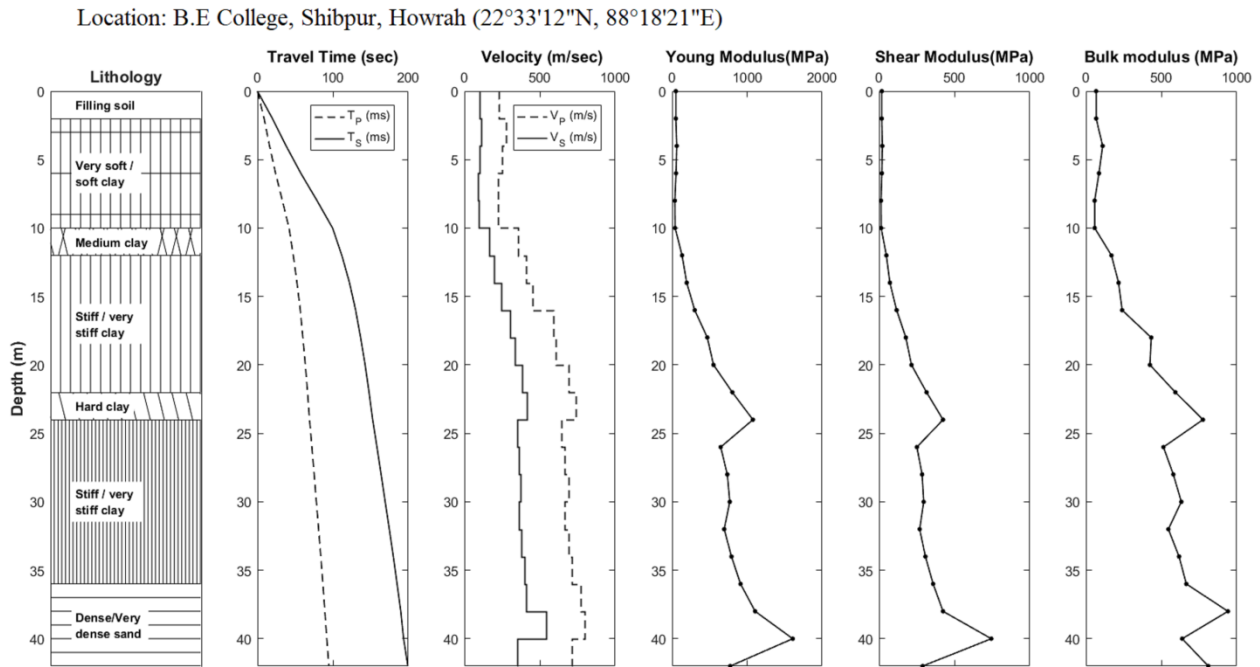


Fig. 5. Representative Downhole investigation carried out at Howrah in West Bengal for the estimation of dynamic physical parameters viz. V_p , V_s , Poisson's Ratio, Young's Modulus, Shear Modulus and Bulk Modulus through P-wave and S-wave travel time picking.

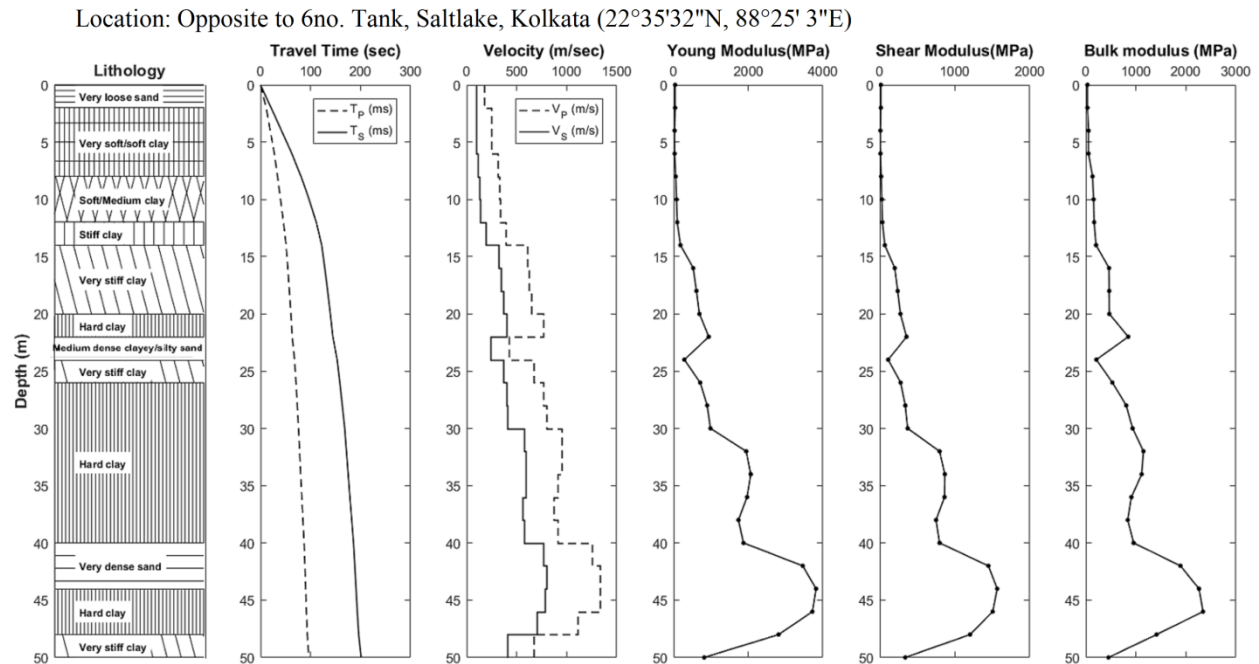


Fig. 6. Representative Downhole investigation carried out at Saltlake city in Kolkata for the estimation of dynamic physical parameters viz. V_p , V_s , Poisson's Ratio, Young's Modulus, Shear Modulus and Bulk Modulus through P-wave and S-wave travel time picking.

3.3, Non-invasive microtremor data acquisition and measurement

The HVSR survey (Horizontal-to-Vertical Spectral Ratio) records natural and anthropogenic microtremors (noise). The spectral ratio of the horizontal component to the vertical component of microtremor record is calculated using the Nakamura Ratio, [30], which assumes that vertical component waves will not change significantly in amplitude, on the other hand, the horizontal component of waves, will be influenced by the properties of soil through which they travel. Resonance frequency due to the local stratigraphic effect is determined by processing the spectral ratio of horizontal and vertical components (HVSR) using the Nakamura relation given in Eq. 2 [30]. Therefore, the H/V ratio is used to estimate

the resonance frequency that causes ground motion amplification when seismic waves are applied, and this amplification can be of the soil/sediment column [30, 31].

$$HVSR = \sqrt{\frac{(NS^2 + EW^2)}{V^2}} \quad (2)$$

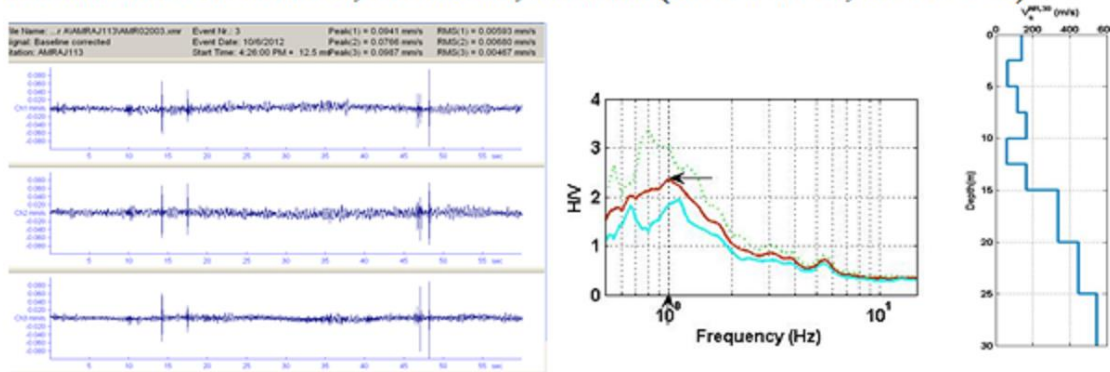
Where NS is the north–south component of amplitude spectrum, EW is the east–west component of amplitude spectrum, and V is the vertical components of amplitude spectrum.

The soil properties and geology of the test site are reflected in the horizontal to vertical response curves derived from the microtremor survey. Microtremor data acquired using SYSCOM MR2000 and TROMINO- 3G at more than 3500 locations throughout the state of West Bengal have

been processed and then inverted using View2002, GEOPSY and GRILLA software to validate the 1D shear wave velocity model derived from geotechnical investigation by comparing the theoretically derived

horizontal to vertical spectral ratio (HVSR) to the observed one. Some representative microtremor data, H/V ratio and the inverted 1D shear wave velocity model at Kolkata and Howrah are depicted in Figure 7.

(a) Location: Near Unitech, Newtown, Kolkata (22°34'41"N, 88°29'1"E)



(b) Location: IEST, Shibpur, Howrah (22°33'27"N, 88°18'24"E)

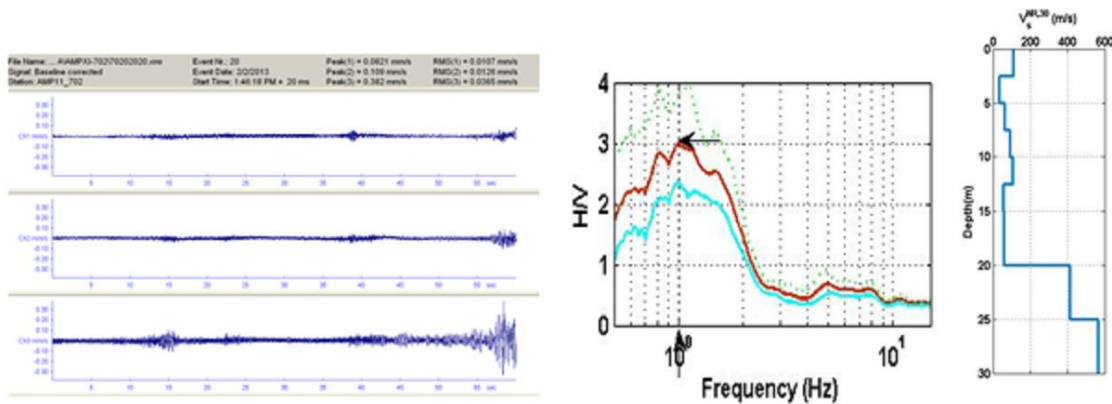


Fig. 7. Representative Ambient noise survey data, computed H/V curves obtained through Nakamura technique and H/V inverted 1D Shear wave velocity structure at (a) Newtown in Kolkata and (b) Shibpur in Howrah.

3.3, Non-invasive SASW and MASW data acquisition and measurement

The Spectral Analysis of Surface Wave (SASW) method estimates the shear wave velocity of sub-surface soil/sediment layers by using the dispersion properties of

Rayleigh waves in a multi-layered medium [32]. An impulsive source generates S-waves, which are detected by geophones. The recorded data is then analyzed in frequency domain to produce a dispersion curve, which is then used to compute a depth-dependent shear wave velocity profile. An expanding

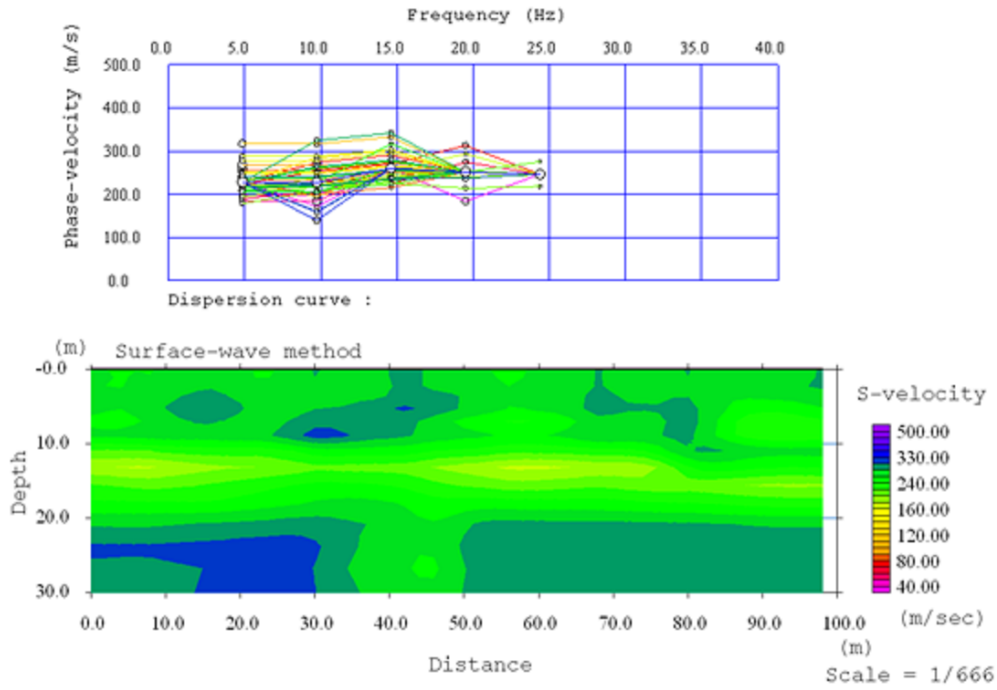
receiver spread is used to avoid the near-field effects caused by Rayleigh waves and the source-receive system. The SASW method concentrated on ways to improve a field procedure which is used to improve the accuracy of the fundamental mode (M_0) Rayleigh wave dispersion curve.

In the recent years, the Multichannel Analysis of Surface Waves (MASW) method has been used in shallow depth engineering studies to estimate the shear wave velocity (V_s)[32]. The dispersive property of Rayleigh waves is used to measure subsoil shear wave velocity, which is a function of the rigidity of the medium in which they travel. Data was collected in the field through forward, center, and/or reverse shots. While evaluating the results, first we obtain the fundamental mode phase velocity from surface wave records and then 1D shear wave

velocity along depth sections is calculated using the damped least squares inversion process.

The SASW dispersion analysis method is based on phase shift as a function of frequency between two receivers while the MASW technique is based on the relationship between phase angles and source to receiver offset [33]. MASW data acquired from McSEIS-SX 48 channel and SOILSPY ROSINA at various locations throughout the state of West Bengal were processed and inverted using SeisImager/SW and GRILLA software to obtain both 1D and 2D subsurface shear wave velocity profiles. Representative 2D shear wave velocity along with their corresponding dispersion curve are shown in Figure 8 and Joint fit of H/V and dispersion curves from MASW survey at Khajra in West Midnapore is shown in Figure 9.

(a) Location: Gorabazar, Dumdum, Kolkata ($22^{\circ}37'58''\text{N}$, $88^{\circ}25'03''\text{E}$)



(b) Location: NH-6, Kona Exp., Howrah ($22^{\circ}37'16''\text{N}$, $88^{\circ}17'25''\text{E}$)

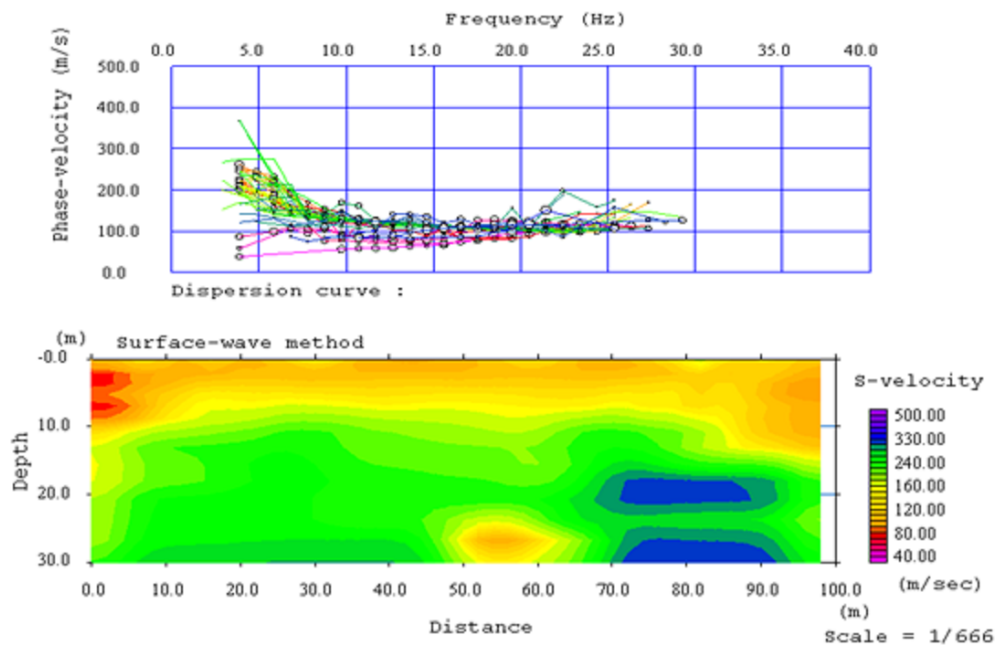


Fig. 8. Representative Dispersion curves through the plotting of phase frequency versus phase velocity derived from MASW survey and phase velocity inverted 2D Shear wave velocity section at (a) Dumdum in Kolkata and (b) Kona Expressway in Howrah.

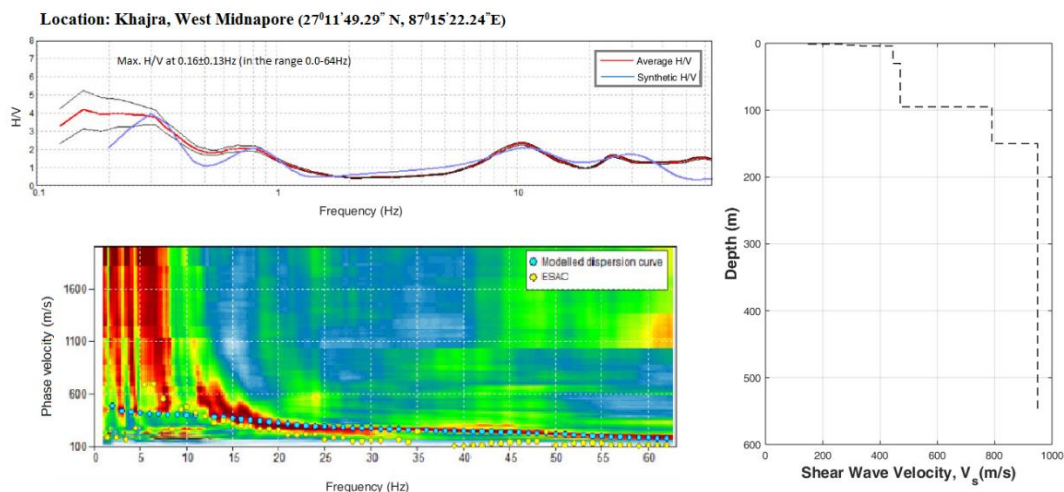


Fig. 9. Representative Joint fit of ambient noise survey derived H/V curves and dispersion curves derived from SASW survey wherein 2D Shear wave velocity section has been derived through joint inversion of dispersion and H/V data model of the subsurface at Khajra, West Midnapore in West Bengal.

4. Site classification of west bengal and kolkata

Effective shear wave velocity (V_s^{30}) is a good indicator of soil stiffness and acoustic impedance contrast across sediment stratum; thus, its spatial distribution can help understanding the presence of various sediment strata in the entire state of West Bengal including its capital city Kolkata thus rendering it an efficient proxy for site classification. An attempt has been made to develop site and lithology-specific empirical correlations between SPT-N and V_s for West Bengal in which four lithological units have been identified. Four generalized equations

have been provided for major lithological units viz. sand, clay, silt and all soils. In order to depict the generalized characteristics of these SPT-N value versus V_s nonlinear regressed equations we presented a comparison between these expressions and those developed by other workers for other parts of the country and also for overseas alluvium filled earthquake prone districts and observed satisfactory correlation amongst all of them as shown in Figures 10 and 11 for sand, clay and silt & all soils thus providing its generalized characteristics so far as Indian alluvium rich earthquake ravaged districts are concerned and even to those in the global litho-stratigraphic perspective of similar nature as listed in Table 2.

Table 2. Relations between SPT-N value and Shear Wave Velocity of different soil types published in various regions of the world which has been used to compare the proposed empirical relation of the state of West Bengal.

Lithology	Reference	Equations	Region
Sand	Pitilakis <i>et al.</i> (1992) ^(a)	$V_s = 162.0 N^{0.17}$	Greece
	Raptakis <i>et al.</i> (1995) ^(a)	$V_s = 123.4 N^{0.29}$	Greece
	Imai (1977) ^(a)	$V_s = 80.6 N^{0.331}$	Japan
	Hasancebi and Ulusay (2007) ^(a)	$V_s = 90.8 N^{0.319}$	Turkey
	Lee (1990) ^(a)	$V_s = 57.4 N^{0.49}$	USA
	Seed and Idriss (1981) ^(a)	$V_s = 61.0 N^{0.50}$	USA
	Hanumantharao and Ramana (2008) ^(a)	$V_s = 79.0 N^{0.434}$	India (Delhi)
	Fumal and Tinsley (1985) ^(a)	$V_s = 5.1N + 152$	USA
Japan Road Association (1980) ^(b)	$V_s = 100 N^{0.33}$	Japan	

	Chein <i>et al.</i> (2000) ^(a)	$V_s=22.0 N^{0.76}$	Western Tehran
	Kirar <i>et al.</i> (2016) ^(c)	$V_s = 100.3 N^{0.338}$	India (Roorkee)
	Anbazhagan and Sitharam (2010) ^(a)	$V_s=57 N^{0.44}$	India (Bangalore)
	Uma Maheswari <i>et al.</i> (2010) ^(a)	$V_s=100.53N^{0.265}$	India (Chennai)
	Nath <i>et al.</i> (2021) ^(d)	$V_s = 92.126N^{0.3234}$	Indo-Gangetic Foredeep (India)
	Present Study	$V_s = 79.018*[(N_1)_{60}]^{0.503}$	This Study(West Bengal)
Clay	Raptakis <i>et al.</i> (1995) ^(a)	$V_s=105.7 N^{0.33}$	Greece
	Hasancebi and Ulusay (2007) ^(a)	$V_s=97.9 N^{0.269}$	Turkey
	Lee (1990) ^(a)	$V_s=114.4 N^{0.31}$	USA
	Fumal and Tinsley (1985) ^(a)	$V_s=5.3 N+134$	USA
	Hanumantharao and Ramana (2008) ^(a)	$V_s = 86 N^{0.420}$	India (Delhi)
	Imai (1977) ^(a)	$V_s=91.0 N^{0.34}$	Japan
	Naik <i>et al.</i> (2014) ^(e)	$V_s=85.49N^{0.412}$	India (Kanpur)
	Kirar <i>et al.</i> (2016) ^(c)	$V_s=90.6 N^{0.341}$	India (Roorkee)
	Anbazhagan and Sitharam (2010) ^(a)	$V_s=80(N)^{0.33}$	India (Bangalore)
	Uma Maheswari <i>et al.</i> (2010) ^(a)	$V_s=89.31N^{0.358}$	India (Chennai)
	Nath <i>et al.</i> (2021) ^(d)	$V_s = 88.326N^{0.3417}$	Indo-Gangetic Foredeep (India)
	Present Study	$V_s = 82.79*[(N_1)_{60}]^{0.507}$	This Study(West Bengal)
Silt	Imai (1977) ^(a)	$V_s=91.0 N^{0.34}$	Japan
	Lee (1990) ^(a)	$V_s = 106 N^{0.32}$	USA
	Seed and Idriss (1981) ^(a)	$V_s=61.0 N^{0.50}$	USA
	Hanumantharao and Ramana (2008) ^(a)	$V_s = 86 N^{0.420}$	India (Delhi)
	Naik <i>et al.</i> (2014) ^(e)	$V_s=77.49N^{0.39}$	India (Kanpur)
	Dikmen (2009) ^(a)	$V_s = 44 N^{0.48}$	Western Taiwan
	Pitilakis <i>et al.</i> (1999) ^(a)	$V_s = 145.6 N^{0.178}$	Greece
	Nath <i>et al.</i> (2021) ^(d)	$V_s=83.392N^{0.3995}$	Indo-Gangetic Foredeep (India)
	Jafri <i>et al.</i> (2002) ^(a)	$V_s = 22.0 N^{0.77}$	South of Tehran
	Present Study	$V_s = 61.12*[(N_1)_{60}]^{0.652}$	This Study(West Bengal)
All Soil	Athanasopoulos (1995) ^(a)	$V_s=107.6 N^{0.36}$	Greece
	Seed and Idriss (1981) ^(a)	$V_s=61.0 N^{0.50}$	USA
	Imai (1977) ^(a)	$V_s=91.0 N^{0.34}$	Japan
	Kirar <i>et al.</i> (2016) ^(c)	$V_s = 99.5N^{0.345}$	India (Roorkee)
	Hanumantharao and Ramana (2008) ^(a)	$V_s = 82.6 N^{0.43}$	India (Delhi)
	Naik <i>et al.</i> (2014) ^(e)	$V_s = 73.53 N^{0.4}$	India (Kanpur)
	Fumal and Tinsley (1985) ^(a)	$V_s=4.3 N +218$	USA
	Lee (1990) ^(a)	$V_s=106N^{0.32}$	USA
	Nath <i>et al.</i> (2021) ^(d)	$VS = 95.926N^{0.3183}$	Indo-Gangetic Foredeep (India)
		Present Study	$V_s = 100.97*[(N_1)_{60}]^{0.0307}$
Taken from (a) Nath [34]; (b) JRA[35]; (c) Kirar <i>et al.</i> [36]; (d) Nath <i>et al.</i> [29]; (e) Naik and Patra [37]			

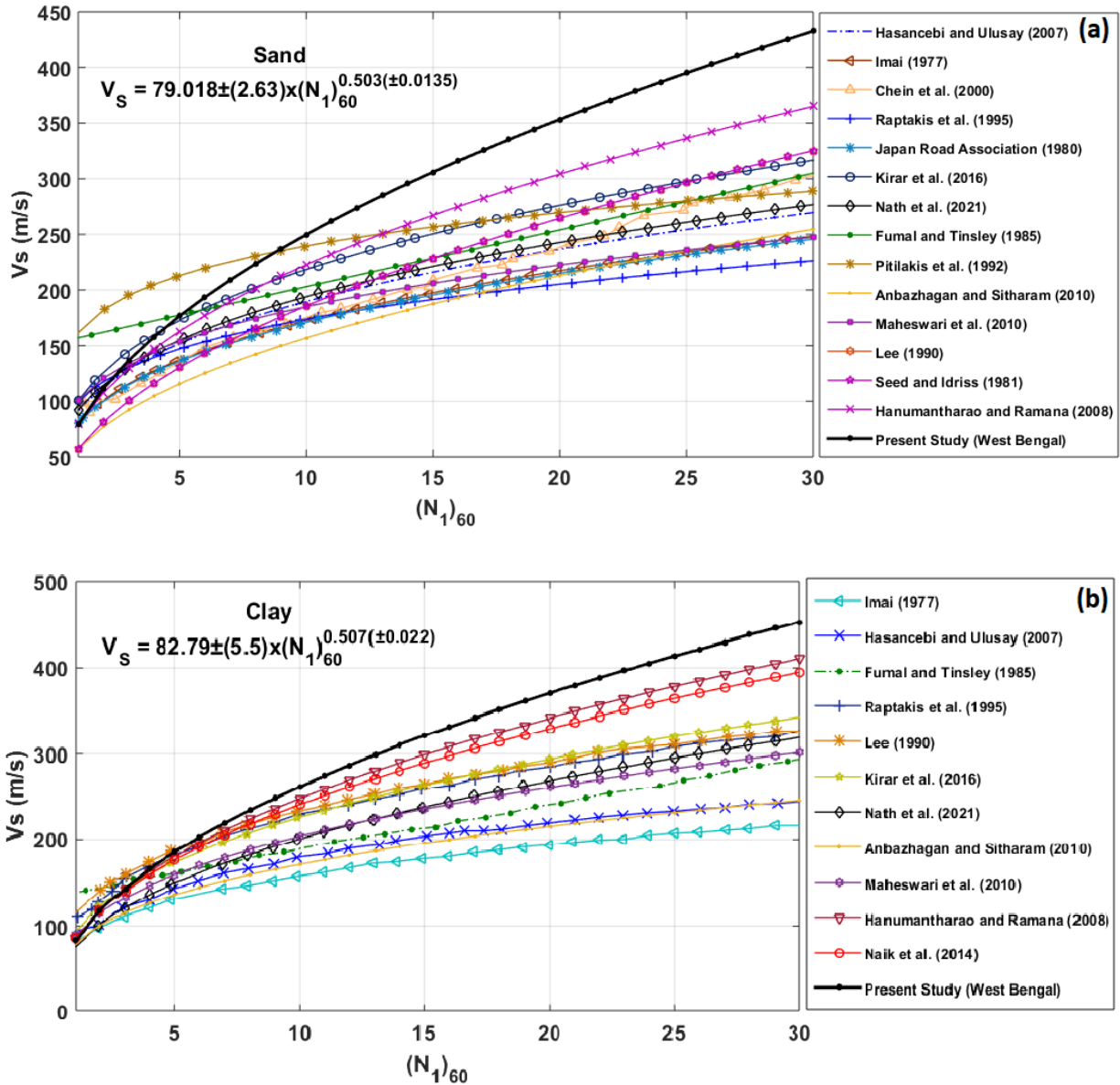


Fig. 10 Comparison of the generated nonlinear empirical power equations for West Bengal with the available empirical relations reported in various literatures for (a) Sand, and (b) Clay depicting satisfactory likelihood in the ensemble.

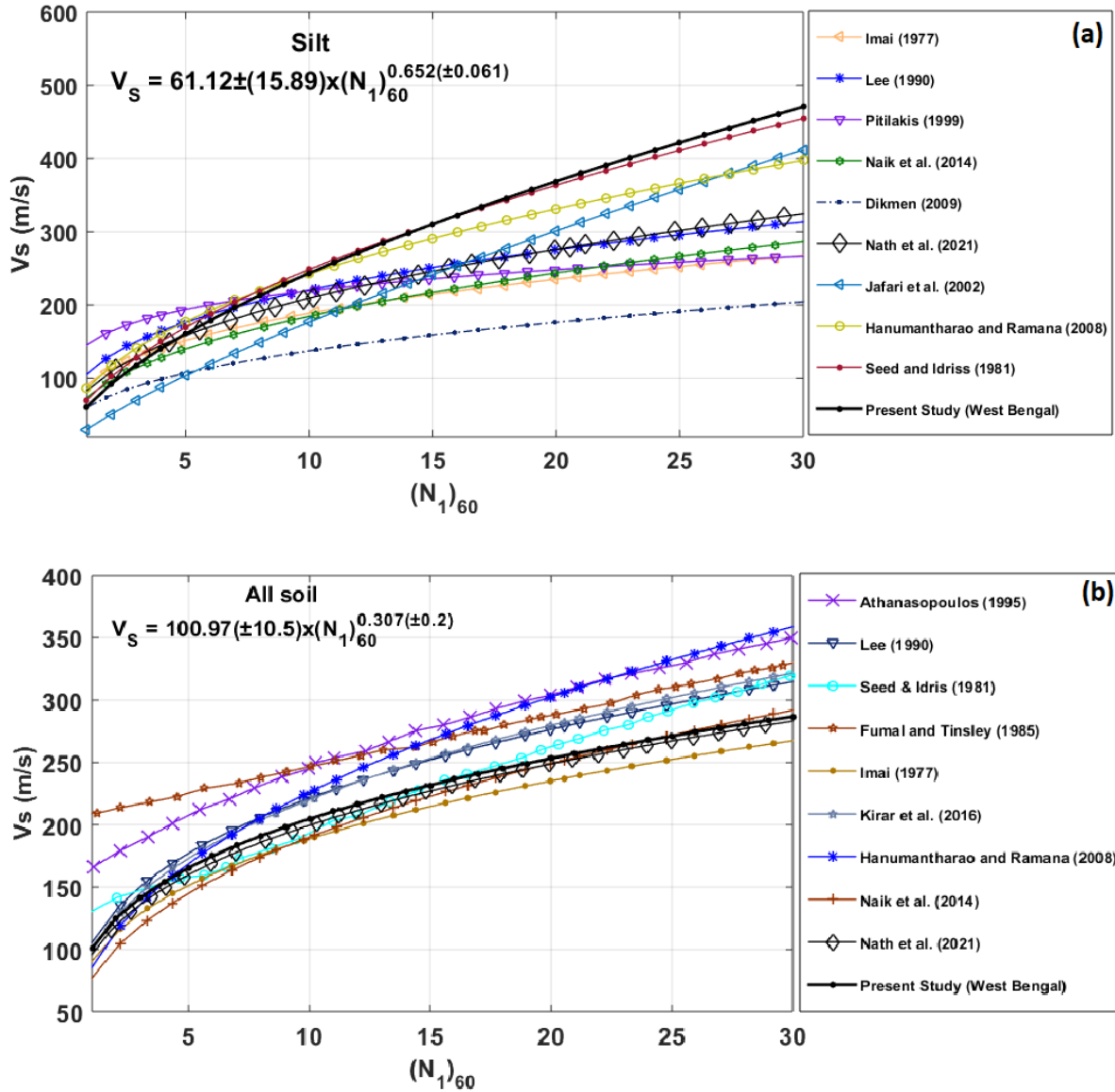


Fig. 11 Comparison of the generated nonlinear empirical power equations for West Bengal with the available empirical relations reported in various literatures for (a) Silt, and (b) All Soils depicting satisfactory likelihood in the ensemble.

National Earthquake Hazard Reduction Program (NEHRP) and Uniform Building Code (UBC [38]) have recommended five site classes for soil/ sediment types based on V_s^{30} with similar site response. Site class A and site class B with $V_s^{30} \geq 1500$ m/s and $1500 > V_s^{30} \geq 760$ m/s respectively are assigned to hard rock and rock site conditions, while site class C is identified with $760 > V_s^{30} \geq$

360 m/s corresponding to soft rock, hard or very stiff soils or gravels, whereas, stiff soils with $360 > V_s^{30} \geq 180$ m/s is designated as site class D [39]. On the other hand, Sun et al. [40] has proposed subdividing site class C and D into four subcategories as: C1 (V_s^{30} : 620-760 m/s), C2 (V_s^{30} : 520-620 m/s), C3 (V_s^{30} : 440-520 m/s), C4 (V_s^{30} : 360-440 m/s), D1 (V_s^{30} : 320-360 m/s), D2 (V_s^{30} : 280-

320m/s), D3 (V_s^{30} : 240-280m/s), D4 (V_s^{30} : 180-240m/s) and E (V_s^{30} <180m/s) respectively.

Site classification map of West Bengal and its Capital Kolkata based on effective V_s distribution is shown in **Figure 12**. The long stretch of the region from Coochbehar to

South 24 Parganas including the city of Kolkata itself exhibits site class E, D4 and D3 belonging to stiff to soft soils/sediments. The city of Kolkata has been pivoted to make it appear in a more expanded view and is delineated to have five site classes ranging from E to D1 (V_s^{30} = 144 to 357m/s).

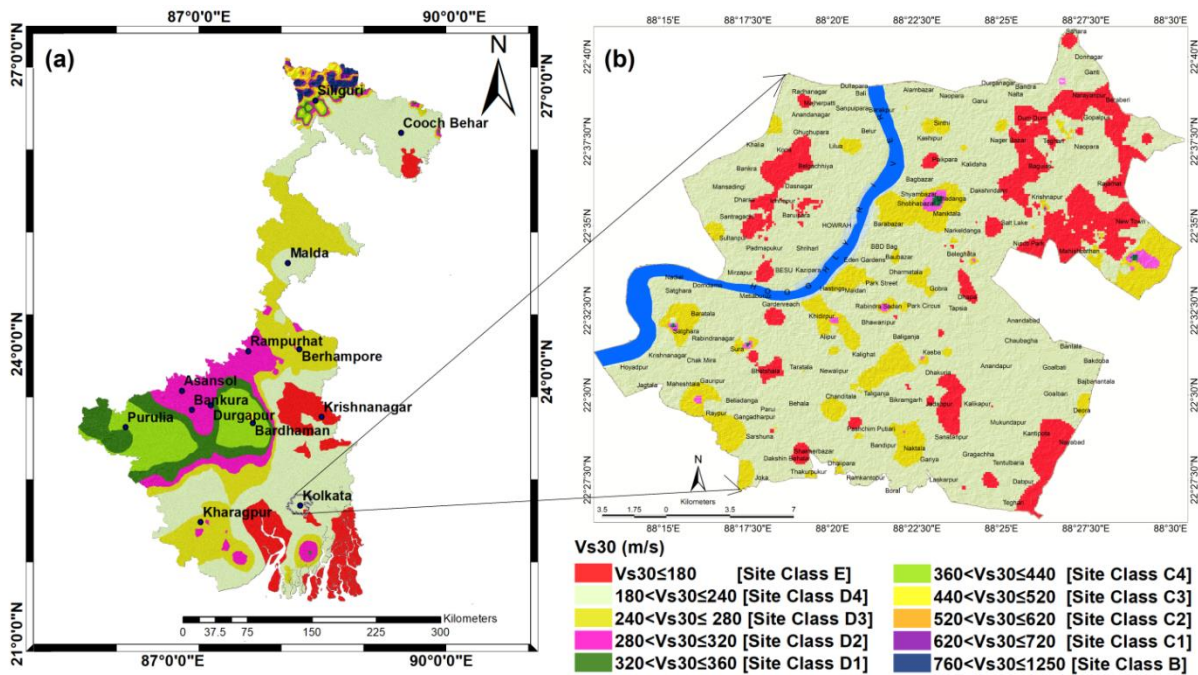


Fig. 12. Site Classification map adhering to Sun nomenclature depicting V_s^{30} distribution in West Bengal and Kolkata [41].

5. Ground motion synthesis of five-great earthquakes from the northeast and eastcentral himalaya

The non-availability of earthquake data, especially for the historic earthquakes, calls for ground motion simulation in a two-step procedure that includes its evaluation at the bedrock and convolution with the local site effects to fetch it to the surface.

5.1. Ground motion at bedrock level

One of the most expedient finite fault stochastic modeling approach has been used

to synthesize ground motion at bedrock through which a filtered and windowed Gaussian white noise is produced whose amplitude spectrum approximates the acceleration spectrum given by physical considerations [16, 42]. The stochastic algorithm uses standard convolution theorem to model spectral acceleration. The amplitude spectrum $A(\omega)$ can be written, in the frequency domain, as the product of source function $SO(\omega, \omega_c)$, a propagation path term $P(\omega)$, and a site function $SI(\omega)$ [16, 42] as given below in Eq. 3,

$$A(\omega) = SO(\omega, \omega_c) \cdot SI(\omega) \cdot P(\omega) \quad (3)$$

Where, $\omega_c = 2\pi f_c$ refers to corner frequency.

The dynamic corner frequency approach [43] facilitates dynamic evolution of corner frequency of the fault rupture, i.e. as the rupture grows frequency content of the radiated seismic wave shifts to lower frequencies. In the stochastic finite-fault simulation technique, a large fault is divided into N number of sub-faults each of which is considered a point source. The ground motion for each sub-fault is calculated by the stochastic point-source method and is summed with a proper time delay in the time domain to obtain the ground motion from the entire fault $A(t)$ as given by Eq. 4 below,

$$A(t) = \sum_{i=1}^{nl} \sum_{j=1}^{nw} H_{ij} * A_{ij}(t - \Delta t_{ij}) \quad (4)$$

Where nl and nw are the number of sub-faults along the length and width of the main fault, H_{ij} is a normalization factor for the ij^{th} sub-fault that aims to conserve energy and Δt is the relative time delay for the radiated wave. For each sub-fault, seismic moment M_{0ij} , corner frequency $f_{c_{ij}}$, and normalization factor H_{ij} need be specified. The moment of the n^{th} sub-fault is calculated using the slip distribution as follows in Eq. 5,

$$M_{0ij} = \frac{M_0 * s_{ij}}{\sum_{i=1}^{nl} \sum_{j=1}^{nw} s_{ij}} \quad (5)$$

Where s_{ij} is the slip of the ij^{th} sub-fault and M_0 is the seismic moment. The dynamic corner frequency is expressed in Eq. 6 as,

$$f_{c_{ij}} = 4.9 * 10^6 N_R(t)^{-1/3} N^{1/3} \beta (\Delta\sigma / M_0)^{1/3} \quad (6)$$

Here $N_R(t)$ is the number of rupture sub-faults at a time t , N refers to total number of sub-faults totaling to $N_R(t)$ at the end of the rupture and $\Delta\sigma$ is the stress drop. The normalization-scaling factor responsible for conserving energy at the high frequency spectral level of the sub-faults is defined by Eq. 7 as,

$$H_{ij} = (N \sum \{f^2 / [1 + (f / f_o)^2]\} / \sum \{f^2 / [1 + (f / f_{oij})^2]\})^{1/2} \quad (7)$$

Where, f_0 is the corner frequency of the entire fault length. The high-frequency energy radiated from all the sub-faults is assumed equal, with the sum being constrained by the total high-frequency energy of the earthquake, as implied by its Fourier spectral acceleration amplitude at high frequencies.

Accelerogram for the largest seismic events triggered in the Central Himalaya and Northeast India viz. 1934 Bihar-Nepal, 1918 Srimangal, 1897 Shillong, 1950 Assam and 2015 Gorkha Nepal earthquakes have been stochastically simulated at the bedrock level at each borehole site by using the parameters taken from [26, 44] as presented in Table 3. The ground motion at bedrock rock for the selected five earthquakes at five different locations of the State is shown in Figure 13.

Table 3. Earthquake source parameters adopted for Strong Ground Motion simulation at West Bengal and Kolkata for 1934 Bihar-Nepal, 1918 Srimangal, 1897 Shillong, 1950 Assam and 2015 Gorkha Nepal earthquakes.

Parameter	1934 Bihar-Nepal Earthquake ^(a)	1918 Srimangal Earthquake ^(b)	1897 Shillong Earthquake ^(c)	1950 Assam Earthquake	2015 Gorkha Nepal Earthquake
Strike	285°	45°	112°	333.5°	96°
Dip	6°	77°	50°	57.5°	79°
Focal depth (km)	20	14	35	35	8.2
Source (Location)	27.55°N, 87.09°E	23.8°N, 90.1°E	26.0°N, 91.0°E	28.38°N, 96.68°E	28.23°N, 84.731°E
Magnitude (M_w)	8.1	7.6	8.1	8.7	7.8
Stress (bar)	275	159	159	66	140
Crustal density (g/cm^3)	2.7	2.7	2.7	2.9	2.8
Shear wave velocity (β) (km/s)	3.8	3.8	3.8	3	3.7
Quality factor	$167f^{0.47}$	$224f^{0.93}$	$372f^{0.72}$	$253f^{0.8}$	$893f^{0.32}$
Kappa	0.02	0.02	0.02	0.02	0.02
Geometrical spreading	1/R (R<100km) 1/R ^{0.5} (R>100km)				
Windowing function	[45]				
Damping	5%				
	(a)[46] (b) [47] (c) [48] (d) [49] and (e) [44]				

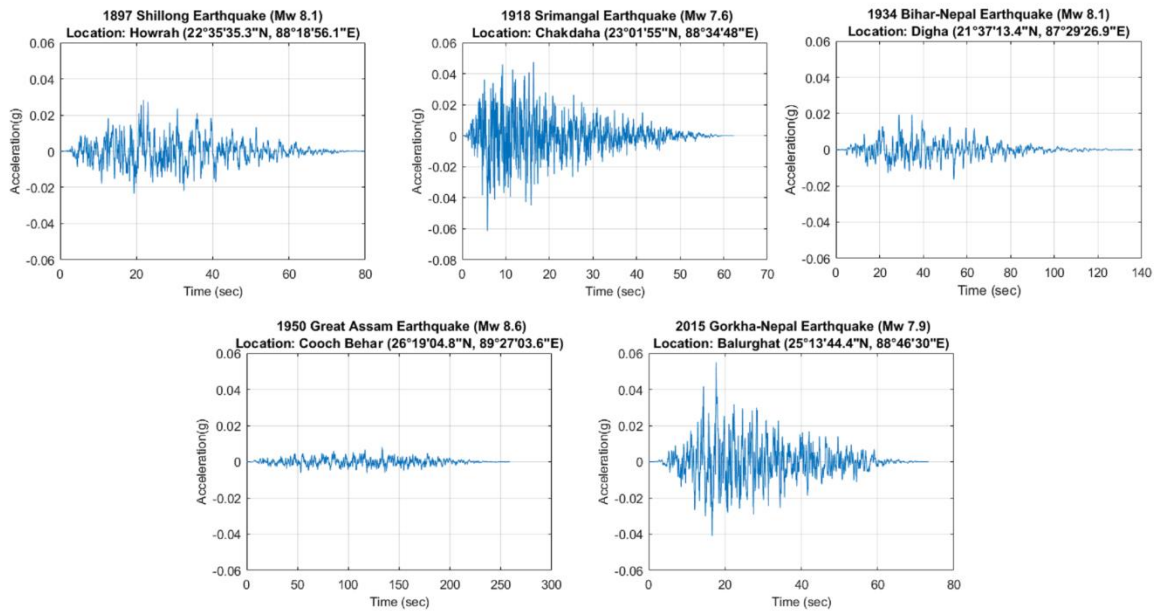


Fig. 13. Strong ground motion simulated through EXSIM at firm rock conditions [Site Class B/C: $V_s \geq 760m/s$] for the 1897 Shillong Earthquake, 1918 Srimangal Earthquake, 1934 Bihar-Nepal Earthquake, 1950 Assam Earthquake and 2015 Gorkha Nepal Earthquake at Howrah, Chakdaha, Digha, Cooch behar and Balurghat in West Bengal.

5.2. Ground motion at the surface

In the proposed work, to assess the effect of sediment layer properties on the propagated ground motions 1D equivalent/quasi-linear approach for site response analysis have been adopted and the computation have been performed by DEEPSOIL [50] which uses the geotechnical parameters as inputs *viz.* soil type, thickness of each layer, unit weight of the material, and shear wave velocity of the material along with the acceleration time history at the engineering bedrock level as inputs. The representative input soil profile and the model input file at Saltlake city in Kolkata is presented in Table 4. The following assumptions have been made during the analysis:

- (a) The soil layers are homogeneous, horizontal and encompass to infinity.
- (b) The ground surface is leveled.
- (c) The incident earthquake motions, which are considered spatially uniform and propagates vertically.

The nonlinear effect of the soil/sediment is approximated by changing the linear elastic properties of the soil as a function of induced

strain level. Thus, the values of strain compatible shear modulus and damping ratio values are iteratively computed based on the estimated strain level. The steps followed in this analysis are as follows [51].

- (1) Estimate Shear modulus (G) and Damping (ζ) for each layer.
- (2) Calculate strain transfer function for each of the layers.
- (3) Compute ground response and shear strain for each layer from the estimated G and ζ .
- (4) Determine effective shear strain in each layer from the maximum shear strain in the time history.
- (5) Recalculate strain compatible shear modulus and damping ratio from the effective strain within each layer.
- (6) Compare new nonlinear properties (G and ζ) with the values obtained in the previous iteration and calculate an error thereof. If the error for all the layers falls below a defined threshold, the computation terminates.

Table 4. Representative DEEPSOIL input and model parameter for a representative site at Saltlake in Kolkata.

Layer	Layer Name	Thickness (m)	Unit Weight (KN/m ³)	Shear Wave Velocity (m/sec)
1	Light grey silty fine sand(filled up)	2.7	16.9	115.06
2	Dark grey clayey silt	0.3	17.1	108.63
3	Dark grey clayey silt	1.725	17.2	104.61
4	Dark grey clayey silt	3	17	140.03
5	Dark grey clayey silt	3	17.4	180.35
6	Dark grey clayey silt	0.775	17.5	218.83
7	Bluish grey silty clay with boulder	2.225	17.4	213.89
8	Bluish grey silty clay with boulder	3	17.7	214.04
9	Bluish grey silty clay with boulder	1.075	18.5	212.15
10	Light yellow with brownish patches silt	1.925	18.6	208.99
11	Light yellow with brownish patches silt	3	18.9	274.04
12	Light yellow with brownish patches silt	3	19	324.68
13	Light yellow with brownish patches silt	3	19.2	365.90
14	Light yellow with brownish patches silt	1.275	20.8	390.21

The stochastically generated input bedrock motions corresponding to 1897 Shillong earthquake of Mw 8.1, 1918 Srimangal earthquake of Mw 7.6, 1934 Bihar-Nepal earthquake of Mw 8.1, 1950 Assam earthquake of Mw 8.7 and 2015 Gorkha Nepal earthquake of Mw 7.8 have been propagated through the soil/sediment column

which includes soil types, thickness of each layer, plasticity index, unit weight and shear wave velocity in each layer. A representative illustration of synthesized bedrock ground motion propagated through 1D lithology to the surface at Saltlake for all the five earthquakes are presented in Figure 14.

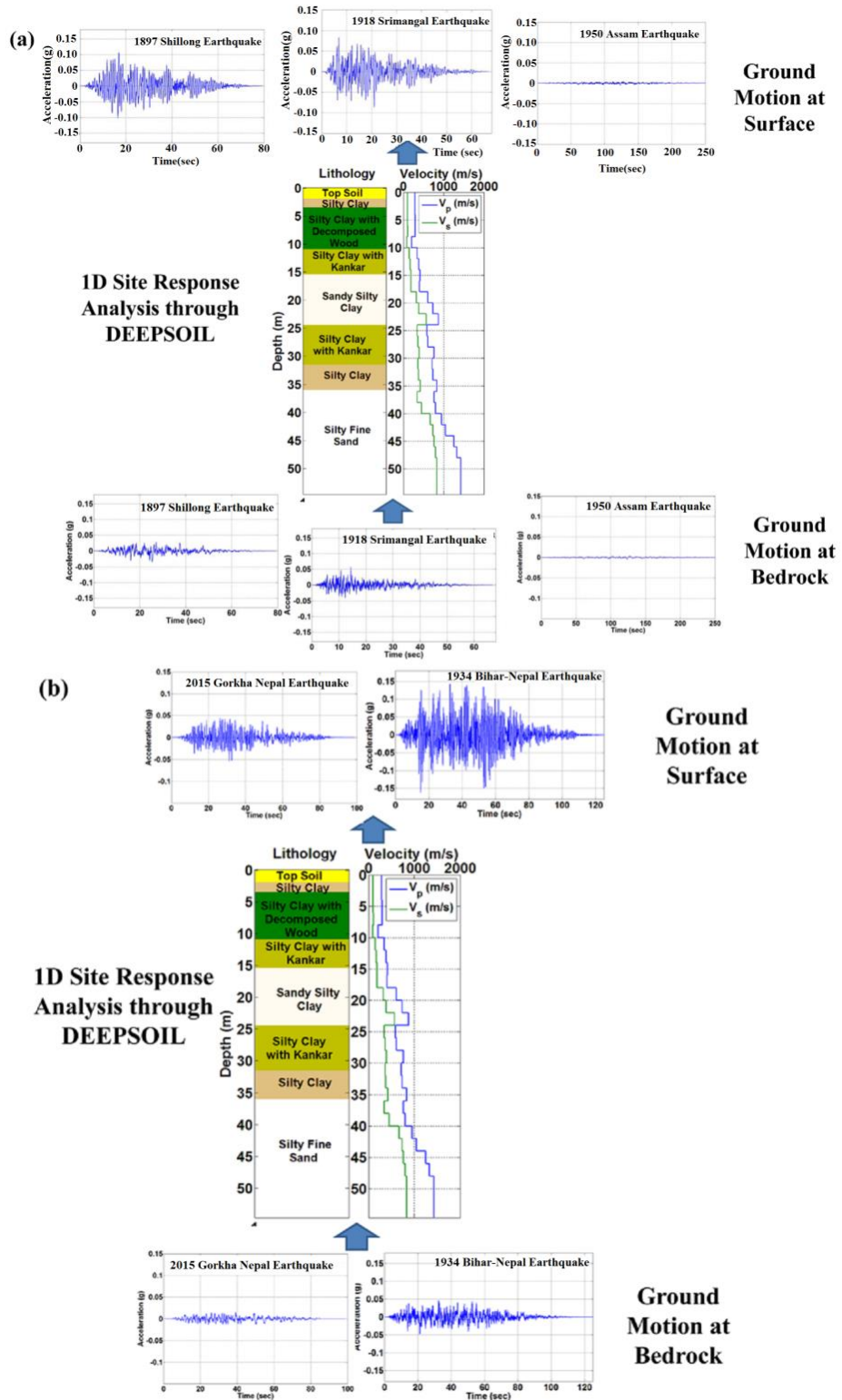


Fig. 14. Depth-wise V_p and V_s , stochastically simulated ground motion at bedrock, the encountered sediment column and ground motion at surface for the five considered earthquake from (a) Northeast India (b) Eastcentral Himalaya.

6. Soil liquefaction susceptibility assessment: algorithm and computation

Soil liquefaction is a critical phenomenon in which seismic shaking reduces strength and stiffness of sediments and the ability of the soil layer to support foundations for structure are decreased. Standard Penetration Test, Cone Penetration Test, Shear Wave Velocity, Resistivity and Capacitance of soil-based liquefaction potential study have already been carried out by several scientists [52–58]. Amongst these, Standard Penetration Test has been established to be an efficient method for the assessment of liquefaction susceptibility of sediments. Correlation between soil SPT resistance and seismic shaking has shown a good agreement during earthquakes in China, Japan and America [53, 59, 60]. However, the liquefaction susceptibility at a site can be identified by calculating Factor of Safety (FOS) values against liquefaction for various soil layers. FOS can be defined as a ratio of cyclic resistance ratio (CRR), which is indicative of the soil resistance to the cyclic stress ratio (CSR) that depends on stresses generated in soil due to seismic loading. A factor of safety value greater than 1.0 indicates that a

particular layer in a soil profile is safe against liquefaction. CRR can be evaluated either from in-situ tests or from laboratory measurements [59] and CSR can be determined from earthquake loading [52]. Many researchers [61, 62] proposed probabilistic method for the analysis of liquefaction potential of any region. According to Juang et al. [63],

liquefaction probability is most suitable for regional mapping purposes. Both liquefaction probability and FOS measure liquefaction for a single layer, therefore, to map this secondary hazard for the entire soil profile Iwasaki [64, 65] introduced Liquefaction Potential Index (LPI) as weighted integral of the product of the thickness of the liquefied layer, closeness of the liquefied layer to the surface and the quantity by which the Factor of Safety is defined [66]. On the other hand, Lee et al. [67] proposed Liquefaction Risk Index (I_R) to map induced ground failure potential of sediments present in the top 20m soil/sediment column. The computational framework with all the computation modules embedded in it for estimating Factor of Safety, Probability of Liquefaction, Liquefaction Potential Index and Liquefaction Risk Index is presented in Figure 15.

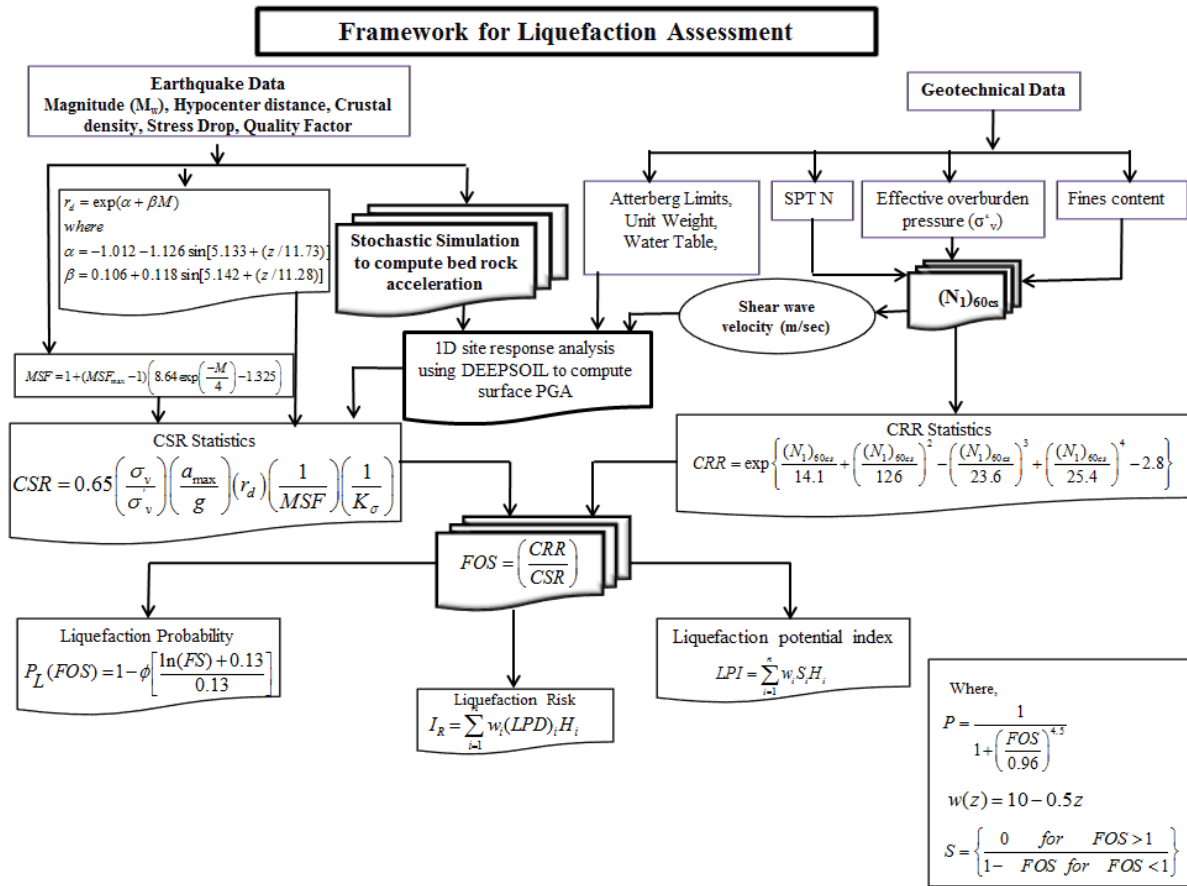


Fig. 15. Computational protocol for soil liquefaction analysis (modified after Nath et al. [26, 66]).

6.1. Liquefaction potential assessment of west bengal and its capital city kolkata

Field observations from various earthquakes around the globe have exhibited that for an earthquake of a given magnitude the occurrence of liquefaction is mostly confined within a particular distance from the epicenter beyond which liquefaction is not observed [68, 69]. Many researchers attempted to establish empirical relation between the earthquake magnitude and the epicentral distance at which liquefaction phenomenon is expected to affect a terrain at the regional scale as well as worldwide. These relations provide an estimate of the minimum energy of an earthquake capable of inducing liquefaction phenomenon [70]. The

maximum epicentral distance at which liquefaction is reported acts as a threshold distance for the liquefaction to occur.

Using Japanese earthquakes and their effects, Kuribayashi and Tatsuoka [71] evaluated the correlation between the maximum epicentral distance at which liquefaction has been exhibited and the associated magnitude and provided the following relation (Eq. 8),

$$\log(R_e) = 0.77(M) - 3.6 \tag{8}$$

Where, epicentral distance R_e is in km. These data were used by Youd [72] and Youd and Perkins [73] along with the other reporting of liquefaction phenomenon to develop upper bound lines for epicentral distance at which liquefaction is supposed to

have been triggered. Based on 40 well-documented earthquakes Keefer [74] suggested exponential increase of distance with increasing magnitude. Subsequently using 137 liquefaction case studies associated with various earthquakes worldwide with liquefaction signature of lateral spreading, reduction of bearing strength and ground settlement, outburst of sand boils and mud volcano, Ambraseys [68] proposed that R_e and moment magnitude, M_w are bounded by a curve with the following empirical Eq. 9,

$$M_w = -0.31 + 2.65 \times 10^{-8} R_e + 0.88 \log(R_e) \quad (9)$$

Where R_e is in km. Papadopoulos and Lefkopoulos [75] modified the data provided by Ambraseys [68] from two American earthquakes (Loma Prieta and Falcon State earthquakes), one from New Zealand (Edgecumbe earthquake) and 30 from Greek earthquakes and updated the proposed equation as given in Eq. 10,

$$M_w = -0.44 + 3 \times 10^{-8} R_e + 0.98 \log(R_e) \quad (10)$$

In this light, all the available global data have been amalgamated with those obtained from the Indian peninsula considering the 1897 Shillong [9, 10], 1918 Srimangal [17], 1934 Bihar-Nepal [13], 1988 Bihar-Nepal [23], 2001 Bhuj [76, 77], 2005 Kashmir [78], and 2015 Gorkha Nepal [79, 80] earthquakes and thereafter plotted in the plane of moment magnitude versus epicentral distance wherever liquefaction signature have been evidenced on which the relationship proposed by Ambraseys [68] is also overlaid in order to draw a boundary between the

liquefiable and non-liquefiable zones as depicted in Figure 16. As exhibited in this diagram the epicentral distance of capital city Kolkata from all the 05 large earthquakes fall in the non-liquefiable zone except for the 1934 Bihar-Nepal earthquake which is observed to have been located on the curve representing the boundary between the two zones. The 1897 Shillong earthquake is also seen to lie in the close proximity of the boundary while the other three earthquakes are seen a bit far.

Therefore, the great historical earthquakes originated from Northeast India and Central Himalaya viz. the 1897 Shillong, 1918 Srimangal, 1934 Bihar-Nepal, 1950 Assam and 2015 Gorkha Nepal earthquakes have been considered to perceive the liquefaction potential of the underlying alluvium below West Bengal and in Kolkata, which have reportedly caused damage to the both due to the impact of soil liquefaction caused by the amplified ground motion combined with shallow ground water condition and the presence of soft alluvial sediments in the state of West Bengal and its capital Kolkata. A detailed liquefaction potential analysis in terms of computation of Factor of Safety (FOS) and Probability of Liquefaction (PL) of the region has been performed to judge as to whether each shallow lithological layer is safe or unsafe. Liquefaction Potential Index (LPI) and Liquefaction Risk Index (IR) have also been estimated to assess the extent of liquefaction for the top 20m thick soil column at each borehole location in the State and its capital city.

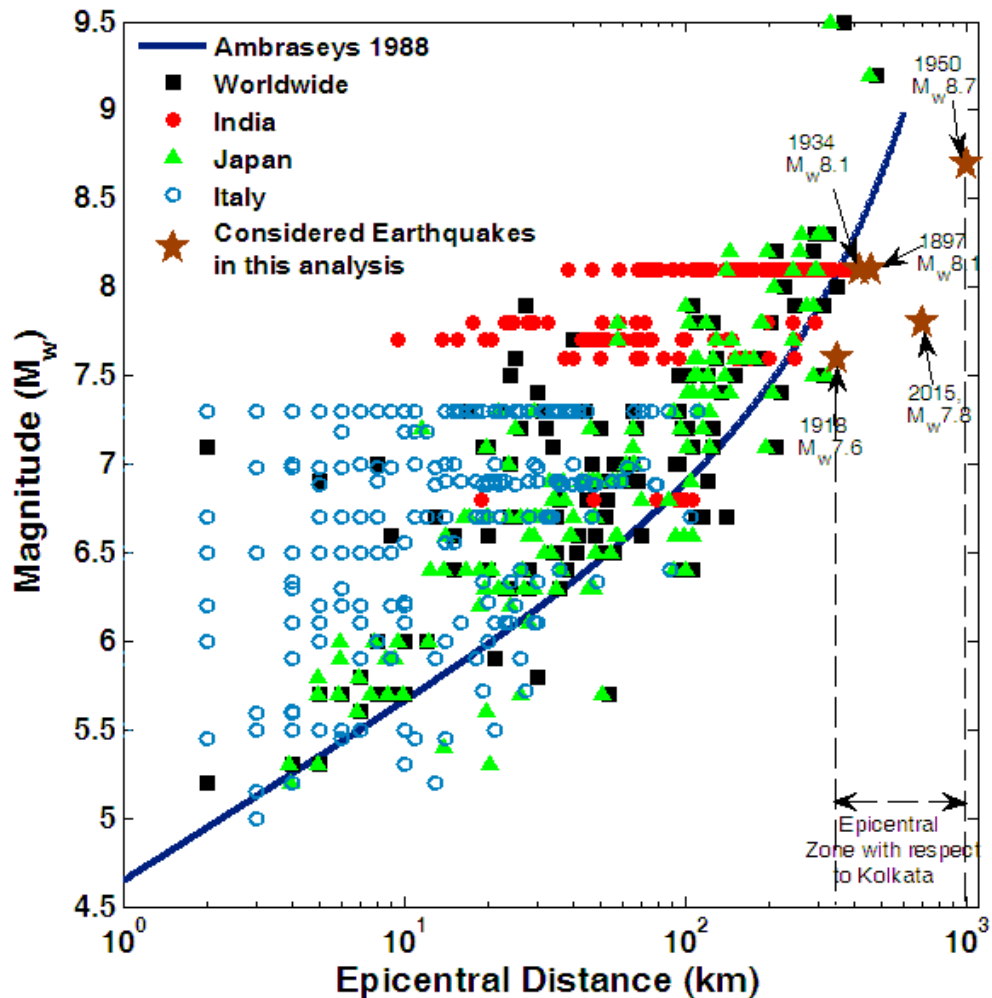


Fig. 16. Demarcation between liquefiable and non-liquefiable zone in the plane of Moment Magnitude (M_w) versus Epicentral distance (R_e) using about 137 worldwide liquefaction signatures. The solid line is the regression relation proposed between M_w and R_e for liquefiable conditions [68].

The liquefaction hazard assessment in the state of West Bengal including its capital city Kolkata inherits the methodology primarily introduced by Seed and Idriss [52] further modified by others [e.g. 3, 80–83] and is based on the database of 3300 boreholes containing information about SPT-N values, shear wave velocity and other index properties *viz.* unit weight, Atterberg limits, percentage of fine

content etc. Physical and shear parameters of sediments as well as the depth of ground water table are considered important criteria for liquefaction susceptibility assessment of a region. The ground water tables for both pre- and post- monsoon periods for both West Bengal and Kolkata as used in this investigation are presented in Figure 17.

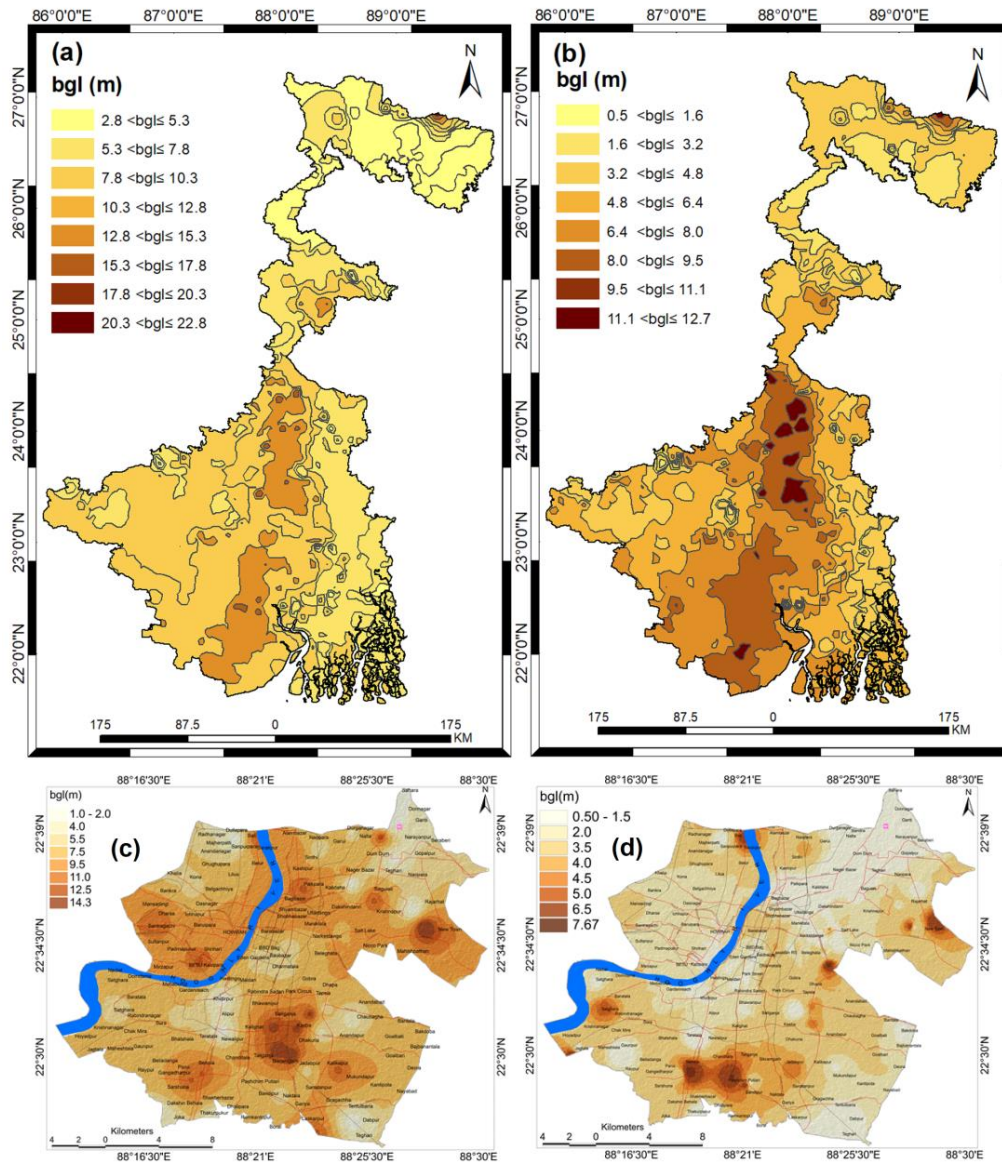


Fig. 17. Spatial distribution of ground water level in the state of West Bengal for both (a) pre-monsoon and (b) post-monsoon period (CGWB, 2018) and that in the city of Kolkata shown in (c-d) respectively.

The CRR profiles with depth for six representative sites, shown in Figure 18 exhibit that CRR values reduce significantly with different water table condition at Berhampore, Chandannagar, Jalpaiguri, Kharagpur, Patharpratima Island in West Bengal and Tollygunge of Kolkata respectively. In addition, it is observed that

there is significant reduction in CRR values by 15%, 13%, 10% and 11% at Shibpur, Park Street, Tollygunge and New Town in Kolkata respectively. Considering the severity of subsurface hazard conditions, only post-monsoon ground water criterion is considered for further analysis.

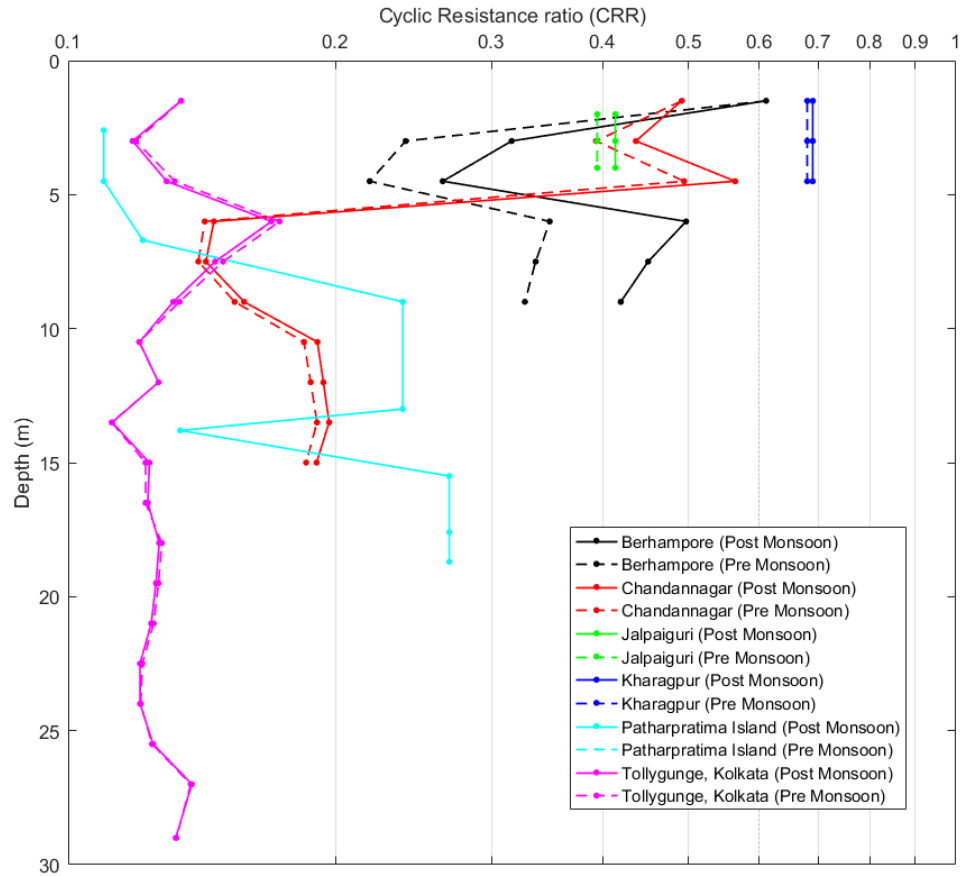


Fig. 18. Depth-wise Cyclic Resistance Ratio (CRR) variation for both pre- and post-monsoon ground water conditions at five representative sites *viz.* Behrampore, Chandannagar, Jalpaiguri, Kharagpur, Patharpratima Island in West Bengal and Tollygunge in Kolkata depicting association of low liquefaction resistance with post-monsoon scenario.

The representative variation of FOS with depth for some Cities in West Bengal including two important landmarks in Kolkata is presented in Figure 19. These plots exhibit that at EM Bypass Dhapa and Park Street in Kolkata and Serampore in West Bengal, the FOS values are less than 1 in the depth range of 5-15m. These areas fall under the site classes E and D4 and also exhibit ground water level of 0.5-12.7m justifying the possibility of liquefaction in this depth range. The liquefaction is attributed to the presence of non-plastic sand and sandy silt/silty sand in the region, as because these coarse-grained sediments hold more water the fine-grained sediments and,

therefore, under the influence of intense ground shaking it is seen to liquefy very easily. It is also evident from these plots that FOS values are higher under the impact of 1950 Assam earthquake successively followed by 2015 Gorkha Nepal earthquake, 1918 Srimangal earthquake, 1897 Shillong earthquake and the 1934 Bihar-Nepal earthquake at all the depth ranges. The sediments at the depth levels of 5-10m and 10-15m are seen to be more prone to liquefaction under the impact of all the five large earthquakes considered here due mostly to the shallow ground water table condition in the State as well as in Kolkata and is seen to vary mostly in at the depth range of 0.50-12.7m.

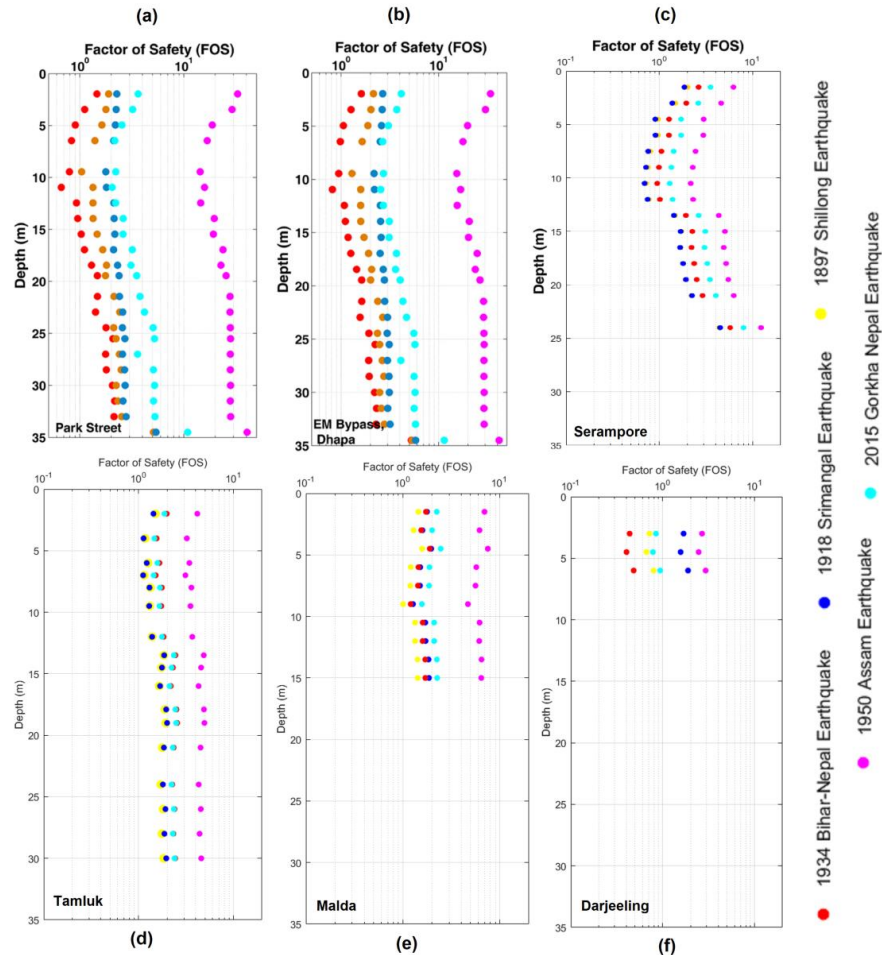


Fig. 19. Depth-wise Factor of Safety variation at (a) Park Street, (b) EM Bypass in Kolkata (c) Srerampore, Hooghly (d) Tamluk (e) Malda and (f) Darjeeling in West Bengal for the 1897 Shillong Earthquake, 1918 Srimangal Earthquake, 1934 Bihar-Nepal Earthquake, 1950 Assam Earthquake and 2015 Gorkha Nepal Earthquake depicting liquefaction phenomena prevalent in 5-15m depth range.

6.2. Liquefaction potential index and liquefaction risk index

Liquefaction Potential Index (LPI) and Liquefaction Risk Index (I_R), estimated by using FOS values of few representative locations in West Bengal for all the five historic earthquakes considered here, which suggest that the State as a whole suffered little from the liquefaction hazard except for some patches in the northeastern territory. A bar graph is presented in Figure 20 to compare the Liquefaction Potential Index (LPI) and Liquefaction Risk Index (I_R) in some selected Cities of the State *viz.*

Serampore, Asansol, Murshidabad, Haldia and Darjeeling for the Scenario earthquakes *e.g.* 1897 Shillong earthquake of M_w 8.1, 1918 Srimangal Earthquake of M_w 7.6, 1934 Bihar Nepal earthquake of M_w 8.1, 1950 Assam earthquake of M_w 8.6 and 2015 Gorkha Nepal earthquake of M_w 7.8. In addition, a synopsis has been presented at a few selected locations in the City *viz.* Saltlake, Dumdum, Park Street and EM Bypass under the impact of these historic earthquakes in Figure 18. It is evident from the presentation that the liquefaction susceptibility and the associated risk have increased significantly with substantial increase in the PGA values. The northern

region of the State is observed to have high LPI and I_R values due to shorter epicentral distances and high PGA values as reported in GSI Memoirs. Southeastern region of the State on the contrary is found to be associated with high LPI and I_R values thus posing high liquefaction risk. Southwestern region of the State on the other hand, presents low LPI and I_R distribution due to its compact soil/sediment lithological composition at shallower depth level. In case

of Kolkata however the northeastern region of the City whose skyline is infested with high-rise concrete buildings and skyscrapers built on an artificial non-engineered fill underlain by decomposed wood/peat, sand lenses and Silty clay/Clayey silt with low SPT-N values is found to be associated with high LPI and I_R values thus posing secondary seismic risk due to severe liquefaction potential.

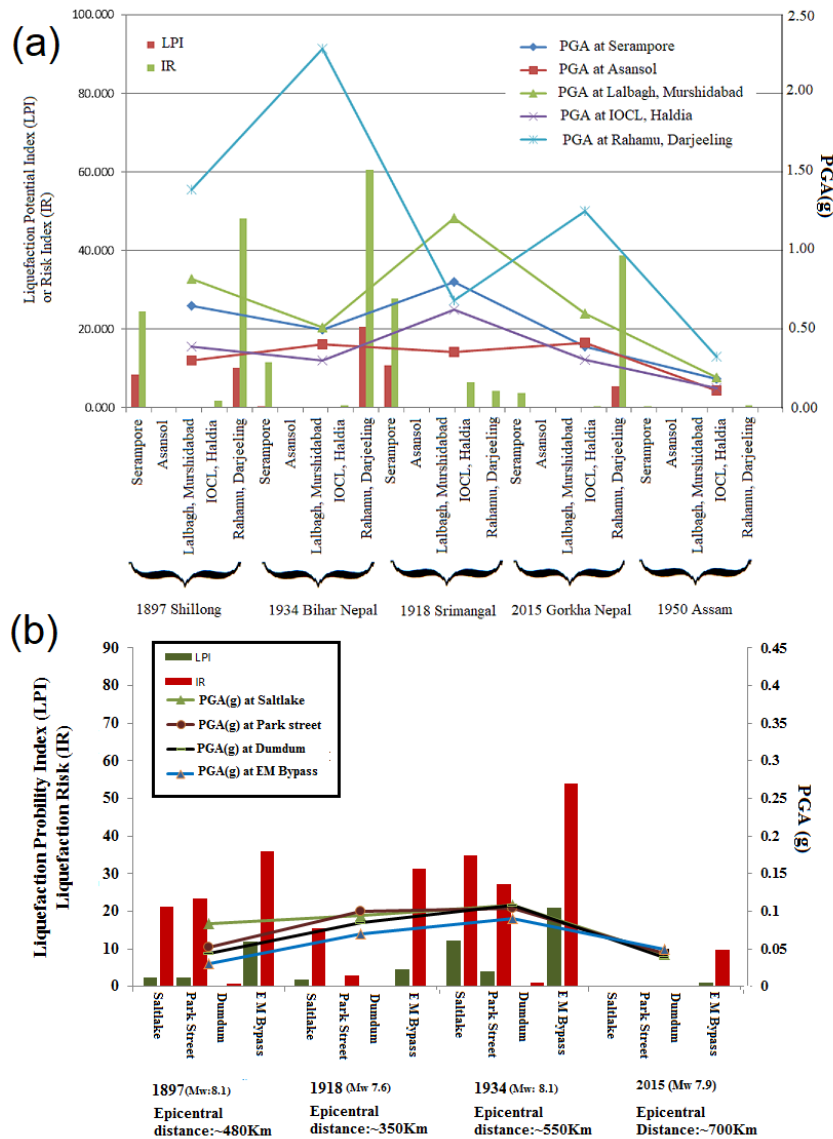


Fig. 20. Bar plot depicting liquefaction potential and Liquefaction Risk Index for the 1897 Shillong Earthquake, 1918 Srimangal Earthquake, 1934 Bihar-Nepal Earthquake, 1950 Assam Earthquake and 2015 Gorkha Nepal Earthquake and associated Peak Ground Acceleration indicated by lines at (a) the state of West Bengal and (b) the city of Kolkata.

The presented results of this study may be used to reduce the risk of ground failure and deformation through various ground improvement techniques like densification, solidification, drainage, dewatering, and reinforcement [84–88].

7. Conclusion

In order to provide a holistic understanding of liquefaction potential and its associated risk, it has been decided to proceed hierarchically starting with site classification based on Ambient Noise Survey, Spectral Analysis of Surface Wave (SASW), Multi-channel Analysis of Surface Wave (MASW), Joint Microtremor & MASW inversion and Geotechnical data at 3300 strategic locations in the state of West Bengal and about 2000 locations in the city of Kolkata where shear wave velocity is estimated in both the lateral and depth-wise varying subsurface lithological units which enabled establishing spatial domain site classification using NEHRP and Sun et al. [41] nomenclature thus dividing the entire terrain into ten site classes of which site class E encompasses most areas of the districts of Nadia, North and South 24 Parganas, East Midnapore, site class D4 is seen in the areas of Coochbehar, Jalpaiguri, Uttar Dinajpur, Malda, Howrah and Hooghly and other parts of North 24 Parganas, parts of East and West Midnapore and site class D3 is seen in most areas of the districts of Malda, Murshidabad and West Midnapore; while site class D4 is dominant in the city of Kolkata with a few patches of site class E prevalent in Dasnagar, Nawabad, Dum Dum and Newtown. Once the site class map of the State as well as the city of Kolkata is prepared, the most logical step will be to characterize it through equivalent linear/nonlinear site response analysis starting with stochastic simulation of strong

ground motion for the 1934 Bihar-Nepal, 1918 Srimangal, 1897 Shillong, 1950 Assam and 2015 Gorkha Nepal earthquakes and use those as input ground motion for the DEEPSOIL package used in the present investigation for spectral response modelling wherein both the Absolute and Spectral Site Amplification as well as depth-wise Pseudo Spectral Acceleration variation and locale-specific surface PGA are established. The simulated Absolute Site Amplification value is seen to vary in the range of 1.04-2.74, while the Predominant Frequency is seen to vary from 0.67Hz to 7.94Hz and the Spectral Amplification Factor varying from 2.28 to 7.56. The surface PGA thus estimated is observed to vary in the range of 0.02-0.27g for the 1934 Bihar-Nepal earthquake, 0.03-0.13g for the 1918 Srimangal earthquake, 0.02-0.13g for the 1897 Shillong earthquake, 0.008-0.045g for the 1950 Assam earthquake and 0.02-0.10g for the 2015 Gorkha Nepal earthquakes with highest PGA observed at Darjeeling, Kalyani, Jalpaiguri and Siliguri respectively. A protocol has been developed for the calculation of Cyclic Stress Ratio (CSR) and Cyclic Resistance Ratio (CRR); based on which Factor of Safety (FOS) values are calculated prompting the determination of Liquefaction Potential Index (LPI), Probability of Liquefaction and Liquefaction Risk Index (I_R) thus classifying the state of West Bengal and its Capital City into ‘Severe’, ‘High’, ‘Moderate’ and ‘Non-’ liquefiable zones while the risk map is produced by categorizing the Liquefaction Risk Index into three classes viz. ‘Low (with: $I_R \leq 20$)’, ‘High (with: $20 < I_R \leq 30$)’ and ‘Extreme (with: $I_R > 30$)’ Risk Zones. It has been noted that many important cities of the State viz. Coal hub of Asansol, Industrial hub of Durgapur, Port City of Haldia, District Towns of Tamruk, Malda, Bankura, Birbhum,

Jhargram, Siliguri, Jalpaiguri are located in the 'Non-liquefiable' zone with $I_R \leq 20$. Darjeeling, the tourist hub of the State belongs to 'Moderate' to 'Severe' liquefiable zone with extreme risk values for the all the earthquakes except the 1950 Assam earthquake. The city of Kalyani has been found to have LPI of 5.5 in case of the 1918 Srimangal earthquake. These observations are found to be in complete agreement with the liquefaction evidences reported in various published literatures and Geological Survey of India Memoirs. In order to delineate the liquefaction susceptibility of the capital city of Kolkata, the Peak Ground Acceleration (PGA) values assessed for the five earthquake scenarios viz. 1897 Shillong (PGA: 0.03-0.11g), 1918 Srimangal (PGA: 0.01-0.10g), 1934 Bihar-Nepal (PGA: 0.05-0.14g), 1950 Assam (PGA: 0.002-0.006g) and 2015 Gorkha Nepal (PGA: 0.01-0.08g) earthquakes have been adapted for the computation of Factor of Safety (FOS) values at every borehole location. For the aforementioned earthquake scenarios, the liquefaction susceptibility mapping suggests that the Northeastern region of the city including the Techno-IT-hub at Saltlake, its new economic hub at Rajarhat and the busiest locations of Central Kolkata encompassing Park Street, Chowringhee etc. are susceptible to liquefaction, while the Southwestern region viz. Alipore is comparatively safe. As far as the subsurface lithostratigraphy is concerned, it can be seen in the plots of Figure 20 that the vulnerability towards liquefaction of the sediment layer in the depth range of 3.5-15 m is high with $FOS < 1$ which may be attributed to the presence of non-plastic sand and sandy silt/silty sand in the region with a groundwater table condition of 0.5-12.7m. These coarse grained sediments have larger

pore size in comparison with the fine sediments which provides more space to retain water which may lead to the vulnerability of the sediment layer to liquefaction under the influence of intense ground shaking due to high PGA. Therefore, the analysis reaffirms that the state of West Bengal and its capital city Kolkata deserve a serious attention towards mitigation and management to be put in place to arrest the earthquake induced liquefaction and its triggered devastations from primary as well as secondary origins.

Acknowledgement

This work has been funded by the Seismology Division of the Ministry of Earth Sciences; Government of India vide sanction order no. MoES/P.O.(Seismo)/1(60)/2009.

Declaration

Ethical statements: We consciously assure that the manuscript contains our own original work, which has not been previously published elsewhere. The paper reflects our own research and analysis in a truthful and complete manner.

Conflicts of interest/Competing interests

The authors declare that there is no conflict of interest.

REFERENCES

- [1] Ambraseys, N., Sarma, S. (1969). "Liquefaction of soils induced by earthquakes." Bulletin of the Seismological Society of America, Vol. 59, Issue. 2, pp. 651–664. doi:10.1785/bssa0590020651.

- [2] Sladen, J. A., D'Hollander, R. D., Krahn, J. (1985). "The liquefaction of sands, a collapse surface approach." *Canadian Geotechnical Journal*, Vol. 22, Issue. 4, pp. 564–578. doi:10.1139/t85-076.
- [3] Youd, T. L., Idriss, I. M., Andrus, R. D., Arango, I., Castro, G., Christian, J. T., Dobry, R., Finn, W. D. L., Jr Harder, L. F., Hynes, M. E., Ishihara, K., Koester, J. P., Liao, S. S. C., Marcuson-III, W. F., Martin, G. R., Mitchell, J. K., Moriwaki, Y., Power, M. S., Robertson, P. K., Seed, R. B., Stokoe-II, K. H. (2001). "Liquefaction Resistance of Soils: Summary Report from the 1996 NCEER and 1998 NCEER/NSF Workshops on Evaluation of Liquefaction Resistance of Soils." *Journal of Geotechnical and Geoenvironmental Engineering*, Vol. 127, pp. 817–833. doi:10.1061/(asce)1090-0241(2001)127:4(297).
- [4] Nath, S. K. (2011). "Seismic Microzonation Manual." Geoscience Division Ministry of Earth Sciences, Government of India.
- [5] USGS. (2008). "USGS Open File Report 2008-1150, Shake out Scenario Appendix C: Characteristics of Earthquake-Induced Permanent Ground Deformation and Examples from Past Earthquakes."
- [6] Holzer, T. L., Bennett, M. J., Ponti, D. J., Tinsley III, J. C. (1999). "Liquefaction and Soil Failure During 1994 Northridge Earthquake." *Journal of Geotechnical and Geoenvironmental Engineering*, Vol. 125, Issue. 6, pp. 438–452. doi:10.1061/(asce)1090-0241(1999)125:6(438).
- [7] Papathanassiou, G., Pavlides, S., Ganas, A. (2005). "The 2003 Lefkada earthquake: Field observations and preliminary microzonation map based on liquefaction potential index for the town of Lefkada." *Engineering Geology*, Vol. 82, pp. 12–31. doi:10.1016/j.enggeo.2005.08.006.
- [8] Shahri, A., Rajablou, R., Ghaderi, A. (2013). "An Improved Method for Seismic Site Characterization with Emphasis on Liquefaction Phenomenon." *Journal of Rehabilitation in Civil Engineering*, Vol. 1, Issue. 1, pp. 53–65. doi:10.22075/jrce.2013.5.
- [9] Oldham, R. D. (1899). "Report on the Great Earthquake of June 12th, 1897." *Geological Survey of India*, Vol. xxix. doi:10.1017/s0016756800174473.
- [10] Ambraseys, N., Bilham, R. (2003). "Reevaluated intensities for the great Assam Earthquake of 12 June 1897, Shillong, India." *Bulletin of the Seismological Society of America*, Vol. 93, Issue. 2, pp. 655–673. doi:10.1785/0120020093.
- [11] Stuart, M. (1921). "The Srimangal Earthquake of 8th July, 1918." *Geological Survey of India Memorandum*, Vol. 46, Issue. 1, pp. 1–70. doi:10.1017/s001675680009097x.
- [12] Sarkar, J. K., Ansary, M. A., Islam, M. R., Safiullah, A. M. M. (2010). "Potential losses for Sylhet, Bangladesh in a repeat of the 1918 Sri- mangal earthquake." *Environmental Economics*, Vol. 1, Issue. 1, pp. 12–31.
- [13] GSI. (1939). "The Bihar-Nepal Earthquake of 1934." *Geological Survey of India*, Vol. 73, pp. 391.
- [14] Lambert, G. (1898). "India, the Horror-Stricken Empire, Containing a Full Account of the Famine, Plague and Earthquake of 1896–7, Including a Complete Narration of the Relief Work through the Home and Foreign Relief

- Commission." Mennonite Publishing Company, Elkhart, Indiana.
- [15] Luttmann-Johnson, H. (1898). "The earthquake in Assam." *Journal of the Society of Arts*, Vol. 46, pp. 473–493.
- [16] Nath, S. K., Raj, A., Thingbaijam, K. K. S., Kumar, A. (2009). "Ground motion synthesis and seismic scenario in Guwahati city-A stochastic approach." *Seismological Research Letters*, Vol. 80, Issue. 2, pp. 233–242. doi:10.1785/gssrl.80.2.233.
- [17] GSI. (1918). "Preliminary note on Srimangal earthquake of July 8, 1918." *Geological Survey of India*, Vol. 3, pp. 173–189.
- [18] GSI. (1934). "Dhubri earthquake 1930." *Geological Survey of India Memorandum*, Vol. 65, pp. 106.
- [19] Gee, E. R. (1934). "The Dhubri earthquake of the 3rd July, 1930." *Office of the Geological Survey*.
- [20] GSI. (1939). "The Bihar-Nepal Earthquake of 1934." *Geological Survey of India*, Vol. 73, pp. 391.
- [21] Dasgupta, S., Pande, P., Ganguly, D., Iqbal, Z., Sanyal, K., Venaktraman, N. V., Dasgupta, S., Sural, B., Harendranath, L., Mazumdar, K., Sanyal, S., Roy, A., Das, L. K., Misra, P. S., Gupta, H. (2000). "Seismotectonic Atlas of India and its Environs." *Geological Survey of India Special Publication*, Vol. 59, pp. 87.
- [22] Kingdon, W. F. (1953). "Flora of Lohit Valley in 1950." *Proceeding of Linnaean Society London*, Vol. 164, pp. 2–8.
- [23] GSI. (1993). "Bihar-Nepal Earthquake, August 20, 1988." *Geological Survey of India*, Vol. 31, pp. 61–81.
- [24] EERI. (2012). "Earthquake Engineering Research Institute: The Mw 6.9 Sikkim-Nepal Border Earthquake of September 18, 2011." *EERI Special Report*.
- [25] Martin, S. S., Hough, S. E., Hung, C. (2015). "Ground motions from the 2015 Mw 7.8 Gorkha, Nepal, Earthquake constrained by a detailed assessment of macroseismic data." *Seismological Research Letters*, Vol. 86, Issue. 6, pp. 1524–1532. doi:10.1785/0220150138.
- [26] Nath, S. K., Adhikari, M. D., Maiti, S. K., Devaraj, N., Srivastava, N., Mohapatra, L. D. (2014). "Earthquake scenario in West Bengal with emphasis on seismic hazard microzonation of the city of Kolkata, India." *Natural Hazards and Earth System Sciences*, Vol. 14, pp. 2549–2575. doi:10.5194/nhess-14-2549-2014.
- [27] Alam, M. K., Hassan, A., Khan, M., Whitney, J. W. (1990). "Geological Map of Bangladesh." *Geological Survey of Bangladesh*.
- [28] GSI. (1999). "Geology and Mineral Resources of the States of India, Pt. 1: West Bengal, Misc." *Geological Survey of India*, Vol. 30, pp. 42.
- [29] Nath, S. K., Ghatak, C., Sengupta, A., Biswas, A., Madan, J., Srivastava, A. (2021). "Regional–Local Hybrid Seismic Hazard and Disaster Modeling of the Five Tectonic Province Ensemble Consisting of Westcentral Himalaya to Northeast India." *Springer Nature Singapore Pte Ltd. 2021*, T. G. Sitharam et Al. (Eds.), *Latest Developments in Geotechnical Earthquake Engineering and Soil Dynamics*, Springer Transactions in Civil and Environmental Engineering, pp. 307–358. doi:10.1007/978-981-16-1468-2_14.
- [30] Nakamura, Y. (1989). "Method for dynamic characteristics estimation of subsurface using microtremor on the ground surface." *Quarterly Report of RTRI*

- (Railway Technical Research Institute (Japan), Vol. 30, Issue. 1.
- [31] Bard, P. Y. (1998). "Microtremor measurement: a tool for site effect estimation?" State-of-the-Art Paper, Proceedings of the Second International Symposium on the Effects of Surface Geology on Seismic Motion, Yokohama, December 1-3, 1998, Irikura, Kudo, Okada and Sasatani (Editors), Balkema, Vol. 3, pp. 1251–1279.
- [32] Park, C. B., Miller, R. D., Xia, J. (1998). "Imaging dispersion curves of surface waves on multi-channel record." 1998 SEG Annual Meeting, 1377–1380. doi:10.1190/1.1820161.
- [33] Nazarian, S., Stokoe, K. H. (1984). "Nondestructive Testing of Pavements using Surface Waves." Transportation Research Record, Vol. 993, pp. 67–79.
- [34] Nath, S. K. (2016). "Seismic Hazard Vulnerability and Risk Microzonation Atlas of Kolkata." Geoscience Division, Ministry of Earth Sciences, ©Govt. of India, New Delhi. <http://www.moes.gov.in/content/seismic-hazard-vulnerability-and-riskmicrozonation-atlas-kolkata>.
- [35] Japan Road Association (JRA). (1980). "Specification and Interpretation of Bridge Design for Highway – Part V: Resilient Design." pp. 14-15.
- [36] Kirar, B., Maheshwari, B. K., Muley, P. (2016). "Correlation Between Shear Wave Velocity (V_s) and SPT Resistance (N) for Roorkee Region." International Journal of Geosynthetics and Ground Engineering, Vol. 2, Issue. 1, pp. 9. doi:10.1007/s40891-016-0047-5.
- [37] Naik, S. P., Patra, N. R. (2018). "Generation of Liquefaction Potential Map for Kanpur City and Allahabad City of Northern India: An Attempt for Liquefaction Hazard Assessment." Geotechnical and Geological Engineering, Vol. 36, Issue. 1, pp. 293–305. doi:10.1007/s10706-017-0327-4.
- [38] UBC. (1997). "Uniform building code." In: International Conference of Building Officials., Whittier, CA.
- [39] Nath, S. K., Thingbaijam, K. K. S. (2011). "Peak ground motion predictions in India: An appraisal for rock sites." Journal of Seismology, Vol. 15, Issue. 2, pp. 295–315. doi:10.1007/s10950-010-9224-5.
- [40] Sun, C. G., Kim, H. S., Chung, C. K., Chi, H. C. (2014). "Spatial zonations for regional assessment of seismic site effects in the Seoul metropolitan area." Soil Dynamics and Earthquake Engineering, Issue. 56, pp. 44–56. doi:10.1016/j.soildyn.2013.10.003.
- [41] Sun, C. G., Kim, H. S., Cho, H. I. (2018). "Geo-proxy-based site classification for regional zonation of seismic site effects in South Korea." Applied Sciences (Switzerland), Vol. 23, pp. 4. doi:10.3390/app8020314.
- [42] Boore, D. M. (1983). "Stochastic simulation of high-frequency ground motions based on seismological models of the radiated spectra." Bulletin of the Seismological Society of America, Vol. 73, pp. 1865–1894.
- [43] Motazedian, D., Atkinson, G. M. (2005). "Stochastic finite-fault modeling based on a dynamic corner frequency." Bulletin of the Seismological Society of America, Vol. 95, Issue. 3, pp. 995–1010. doi:10.1785/0120030207.
- [44] Raghu Kanth, S. T. G., Sreelatha, S., Dash, S. K. (2008). "Ground motion estimation at

- Guwahati city for an Mw 8.1 earthquake in the Shillong plateau." *Tectonophysics*, Vol. 448, Issue. 1–4, pp. 98–114. doi:10.1016/j.tecto.2007.11.028.
- [45] Rodolfo Saragoni, G., Hart, G. C. (1973). "Simulation of artificial earthquakes." *Earthquake Engineering & Structural Dynamics*, Vol. 2, pp. 249–268. doi:10.1002/eqe.4290020305.
- [46] Nath, S. K., Thingbaijam, K. K. S., Vyas, J. C., Sengupta, P., Dev, S. M. S. P. (2010). "Macroseismic-driven site effects in the Southern Territory of West Bengal, India." *Seismological Research Letters*, Vol. 81, Issue. 3, pp. 480–487. doi:10.1785/gssrl.81.3.480.
- [47] Raghu Kanth, S. T. G., Dash, S. K. (2010). "Deterministic seismic scenarios for North East India." *Journal of Seismology*, Vol. 14, pp. 143–167. doi:10.1007/s10950-009-9158-y.
- [48] Hough, S. E., Bilham, R. (2008). "Site response of the Ganges basin inferred from re-evaluated macro-seismic observations from the 1897 Shillong, 1905 Kangra, and 1934 Nepal earthquakes." *Journal of Earth System Science*, Vol. 117, pp. 773–782.
- [49] Dhanya, J., Gade, M., Raghukanth, S. T. G. (2017). "Ground motion estimation during 25th April 2015 Nepal earthquake." *Acta Geodaetica et Geophysica*, Vol. 52, pp. 69–93. doi:10.1007/s40328-016-0170-8.
- [50] Hashash, Y. M. A., Groholski, D. R., Phillips, C. A., Park, D., Musgrove, M. (2011). "DEEPSOIL 5.0, user Manual and Tutorial." University of Illinois, Urbana, IL, USA.
- [51] Kramer, S. L. (1996). "Geotechnical Earthquake Engineering." Prentice Hall, Upper Saddle River, NJ, USA.
- [52] Seed, H. B., Idriss, I. M. (1971). "Simplified procedure for evaluating soil liquefaction potential." *ASCE J Soil Mech Found Div*, Vol. 97, Issue. 9, pp. 1249–1273. doi:10.1061/jsfeaq.0001662.
- [53] Seed, H. B., Idriss, I. M., Arango, I. (1983). "Evaluation of liquefaction potential using field performance data." *Journal of Geotechnical Engineering*, Vol. 3, pp. 109. doi:10.1061/(ASCE)0733-9410(1983)109:3(458).
- [54] Ishihara, K. (1985). "Stability of natural deposits during earthquakes." *Proc. 11th International Conference on Soil Mechanics and Foundation Engineering*, San Francisco, August 1985. Vol. 1, (Balkema).
- [55] Douglas, B. J., Olsen, R. S., Martin, G. R. (1981). "Evaluation of the Cone Penetrometer Test for Use in SPT-Liquefaction Potential Assessment." *ASCE National Convention, Session on In-Situ Testing to Evaluate Liquefaction Susceptibility*, ASCE National Convention, St. Louis, Missouri.
- [56] Robertson, P. K., Campanella, R. G., Wightman, A. (1983). "SPT-CPT correlations." *Journal of Geotechnical Engineering*, Vol. 109, Issue. 11, pp. 1449–1459. doi:10.1061/(ASCE)0733-9410(1983)109:11(1449).
- [57] Campanella, R. G., Robertson, P. K. (1984). "A seismic cone penetrometer to measure engineering properties of soil." 1984 SEG Annual Meeting, SEG 1984, pp. 138–141. doi:10.1190/1.1894361.
- [58] Arulmoli, K., Arulanandan, K., Seed, H. B. (1985). "New method for evaluating liquefaction potential." *Journal of Geotechnical Engineering*, Vol. 111, Issue. 1. doi:10.1061/(ASCE)0733-9410(1985)111:1(95).

- [59] Tokimatsu, K., Yoshimi, Y. (1983). "Empirical Correlation of Soil Liquefaction based on SPT N-value and Fines Content." *Soils and Foundations*, Vol. 23, pp. 4. doi:10.3208/sandf1972.23.4_56
- [60] Seed, H. B., Tokimatsu, K., Harder, L. F., Chung, R. M. (1985). "Influence of SPT procedures in soil liquefaction resistance evaluations." *Journal of Geotechnical Engineering*, Vol. 111, Issue. 12, pp. 1425–1445. doi:10.1061/(ASCE)0733-9410(1985)111:12(1425).
- [61] Yegian, M. K., Whitman, R. V. (1978). "Risk analysis for ground failure by liquefaction." *ASCE J Geotech Eng Div*, Vol. 104, Issue. 7, pp. 921–938. doi:10.1061/ajgeb6.0000672.
- [62] Liao, S. S. C., Veneziano, D., Whitman, R. V. (1988). "Regression models for evaluating liquefaction probability." *Journal of Geotechnical Engineering*, Vol. 114, Issue. 4, pp. 389–411. doi:10.1061/(ASCE)0733-9410(1988)114:4(389).
- [63] Juang, C. H., Ching, J., Luo, Z., Ku, C. S. (2012). "New models for probability of liquefaction using standard penetration tests based on an updated database of case histories." *Engineering Geology*, Vol. 133, pp. 85–93. doi:10.1016/j.enggeo.2012.02.015.
- [64] Iwasaki, T., Tatsuoka, F., Tokida, K., Yasuda, S. (1978). "A practical method for assessing soil liquefaction potential based on case studies at various sites in Japan." *Proceedings of the 2nd International Conference on Microzonation for Safer Construction-Research and Application*, San Francisco, California, USA, pp. 885–896.
- [65] Iwasaki, T., Tokida, K., Tatsuoka, F., Watanabe, S., Yasuda, S., Sato, H. (1982). "Microzonation for soil liquefaction potential using simplified methods." *Third International Earthquake Microzonation Conference Proceedings*, Vol. 3, pp. 1319–1330.
- [66] Nath, S. K., Srivastava, N., Ghatak, C., Adhikari, M. Das, Ghosh, A., Sinha Ray, S. P. (2018). "Earthquake induced liquefaction hazard, probability and risk assessment in the city of Kolkata, India: its historical perspective and deterministic scenario." *Journal of Seismology*, Vol. 22, pp. 35–68. doi:10.1007/s10950-017-9691-z.
- [67] Lee, D. H., Ku, C. S., Yuan, H. (2004). "A study of the liquefaction risk potential at Yuanlin, Taiwan." *Engineering Geology*, Vol. 71, Issue. 1–2, pp. 97–117. doi:10.1016/S0013-7952(03)00128-5.
- [68] Ambraseys, N. N. (1988). "Engineering seismology: Part II." *Earthquake Engineering & Structural Dynamics*. doi:10.1002/eqe.4290170102.
- [69] Wang, C. Y., Manga, M., Wong, A. (2005). "Floods on Mars released from groundwater by impact." *Icarus*, Vol. 175, Issue. 2, pp. 551–5. doi:10.1016/j.icarus.2004.12.003.
- [70] C. Pirrotta, M. S. Barbano, P. Guarnieri, F. Gerardi. (2007). "A new dataset and empirical relationships between magnitude/intensity and epicentral distance for liquefaction in central-eastern Sicily." *Annals of Geophysics*, Vol. 50, Issue. 6. doi:10.4401/ag-3055.
- [71] Kuribayashi, E., Tatsuoka, F. (1975). "Brief Review of Liquefaction During Earthquakes in Japan." *Soils and Foundations*, Vol. 15, Issue. 4, pp. 81–92. doi:10.3208/sandf1972.15.4_81.

- [72] Youd, T. L. (1977). "Packing Changes and Liquefaction Susceptibility." *Journal of the Geotechnical Engineering Division*, Vol. 103, Issue. 8, pp. 918–922. doi:10.1061/ajgeb6.0000478.
- [73] Youd, T. L., Perkins, D. M. (1978). "Mapping liquefaction-induced ground failure potential." *ASCE J Geotech Eng Div*, Vol. 104, pp. 433–446. doi:10.1061/ajgeb6.0000612.
- [74] Keefer, D. K. (1984). "Landslides caused by earthquakes." *Bulletin of the Geological Society of America*, Vol. 95, Issue. 4, pp. 406–421. doi:10.1130/0016-7606(1984)95<406:lcb>2.0.co;2.
- [75] Papadopoulos, G. A., Lefkopoulos, G. (1993). "Magnitude-distance relations for liquefaction in soil from earthquakes." *Bulletin - Seismological Society of America*, Vol. 83, Issue. 3, pp. 925–38. doi:10.1785/bssa0840062019.
- [76] Hough, S. E., Martin, S., Bilham, R., Atkinson, G. M. (2002). "The 26 January 2001 M 7.6 Bhuj, India, earthquake: Observed and predicted ground motions." *Bulletin of the Seismological Society of America*, Vol. 92, Issue. 6, pp. 2061–79. doi:10.1785/0120010260.
- [77] Singh, A. P., Shukla, A., Kumar, M. R., Thakkar, M. G. (2017). "Characterizing surface geology, liquefaction potential, and maximum intensity in the kachchh seismic zone, western India, through microtremor analysis." *Bulletin of the Seismological Society of America*, Vol. 107, Issue. 3, pp. 1277–92. doi:10.1785/0120160264.
- [78] Malik, N. Z., Muhammad, A., Mirza, S. N. (2007). "Phytosociological Attributes of Different Plant Communities of Pir Chinasi Hills of Azad Jammu and Kashmir." *International Journal of Agriculture & Biology*, Vol. 9, Issue. 4, pp. 569–74.
- [79] Subedi, M., Acharya, I. P., Sharma, K., Adhikari, K. (2016). "Liquefaction of Soil in Kathmandu Valley from the 2015 Gorkha, Nepal, Earthquake." *Gorkha Earthquake 2015 Special*, Nepal Engineering Association, pp. 108–115.
- [80] Gautam, D. (2017). "Unearthed lessons of 25 April 2015 Gorkha earthquake (MW 7.8): geotechnical earthquake engineering perspectives." *Geomatics, Natural Hazards and Risk*, pp. 1–25. doi:10.1080/19475705.2017.1337653.
- [81] Idriss, I. M., Boulanger, R. W. (2006). "Semi-empirical procedures for evaluating liquefaction potential during earthquakes." *Soil Dynamics and Earthquake Engineering*, Vol. 26, Issue. 2–4, pp. 115–130. doi:10.1016/j.soildyn.2004.11.023.
- [82] Idriss, I. M., Boulanger, R. W. (2010). "Spt-based liquification triggering procedures." Report UCD/CGM-10/02.
- [83] Boulanger, RW and Idriss, I. M. (2014). "CPT and SPT Based Liquefaction Triggering Procedures." Center for Geotechnical Modeling, Rep. No. UCD/CGM-14 1.
- [84] Andrus, R. D., Chung, R. M. (1995). "Ground Improvement Techniques for Liquefaction Remediation Near Existing Lifelines." Building and Fire Research Laboratory, National Institute of Standards and Technology. U.S. Department of Commerce.
- [85] Ledbetter, R. H. (1985). "Improvement of liquefiable foundation conditions beneath existing structures" Technical Report - US Army Engineer Waterways Experiment Station, Vicksburg, Mississippi.
- [86] National Research Council. (1985). "Liquefaction of Soils during Earthquakes, Committee on Earthquake Engineering."

National Research Council, National Academy Press, Washington.

- [87] Kramer, S. L., Holtz, R. D. (1991). "Soil improvement and foundation remediation with emphasis on seismic hazards." National Science Foundation, Seattle, Washington, pp. 106.
- [88] JSSMFE. (1995). "Remedial Measure Against Soil Liquefaction--From Investigation and Design to Implementation." Japanese Society for Soil Mechanics and Foundation Engineering. (in Japanese, Translation into English in Progress).